NASA/TM-2010-216210

Ares I-X Flight Test Vehicle: Stack 1 Modal Test

Ralph D. Buehrle, Justin D. Templeton, Mercedes C. Reaves, Lucas G. Horta, and James L. Gaspar
Langley Research Center, Hampton, Virginia

Paul A. Bartolotta
Glenn Research Center, Cleveland, Ohio

Russel A. Parks and Daniel R. Lazor
Marshall Space Flight Center, Huntsville, Alabama

March 2010

NASA STI Program . . . in Profile

Since its founding, NASA has been dedicated to the advancement of aeronautics and space science. The NASA scientific and technical information (STI) program plays a key part in helping NASA maintain this important role.

The NASA STI program operates under the auspices of the Agency Chief Information Officer. It collects, organizes, provides for archiving, and disseminates NASA's STI. The NASA STI program provides access to the NASA Aeronautics and Space Database and its public interface, the NASA Technical Report Server, thus providing one of the largest collections of aeronautical and space science STI in the world. Results are published in both non-NASA channels and by NASA in the NASA STI Report Series, which includes the following report types:

- TECHNICAL PUBLICATION. Reports of completed research or a major significant phase of research that present the results of NASA programs and include extensive data or theoretical analysis. Includes compilations of significant scientific and technical data and information deemed to be of continuing reference value. NASA counterpart of peer-reviewed formal professional papers, but having less stringent limitations on manuscript length and extent of graphic presentations.

- TECHNICAL MEMORANDUM. Scientific and technical findings that are preliminary or of specialized interest, e.g., quick release reports, working papers, and bibliographies that contain minimal annotation. Does not contain extensive analysis.

- CONTRACTOR REPORT. Scientific and technical findings by NASA-sponsored contractors and grantees.

- CONFERENCE PUBLICATION. Collected papers from scientific and technical conferences, symposia, seminars, or other meetings sponsored or co-sponsored by NASA.

- SPECIAL PUBLICATION. Scientific, technical, or historical information from NASA programs, projects, and missions, often concerned with subjects having substantial public interest.

- TECHNICAL TRANSLATION. English-language translations of foreign scientific and technical material pertinent to NASA's mission.

Specialized services also include creating custom thesauri, building customized databases, and organizing and publishing research results.

For more information about the NASA STI program, see the following:

- Access the NASA STI program home page at *http://www.sti.nasa.gov*

- E-mail your question via the Internet to help@sti.nasa.gov

- Fax your question to the NASA STI Help Desk at 443-757-5803

- Phone the NASA STI Help Desk at 443-757-5802

- Write to:
  NASA STI Help Desk
  NASA Center for AeroSpace Information
  7115 Standard Drive
  Hanover, MD 21076-1320

NASA/TM-2010-216210

Ares I-X Flight Test Vehicle: Stack 1 Modal Test

Ralph D. Buehrle, Justin D. Templeton, Mercedes C. Reaves, Lucas G. Horta, and James L. Gaspar
Langley Research Center, Hampton, Virginia

Paul A. Bartolotta
Glenn Research Center, Cleveland, Ohio

Russel A. Parks and Daniel R. Lazor
Marshall Space Flight Center, Huntsville, Alabama

National Aeronautics and
Space Administration

Langley Research Center
Hampton, Virginia 23681-2199

March 2010

Acknowledgments

Thanks go to Winifred Feldhaus of NASA Langley Research Center for her assistance with finite element model development. The test execution phase at Kennedy Space Center (KSC) could not have been done without the support of many individuals. Special thanks go to the KSC instrumentation team led by Frank Walker. Logistics and test hardware integration went smoothly due to the dedicated KSC crew that included Russ Brucker, Trip Healey, Stephanie Heffernan, Teresa Kinney, Todd Reeves, Kara Schmitt, Mark Tillett, and Jim Wiltse. Lastly, thanks to our independent verification team of Jeff Lollock, Ryan Tuttle, and Joshua Hwung from Aerospace Corporation.

Available from:

NASA Center for AeroSpace Information
7115 Standard Drive
Hanover, MD 21076-1320
443-757-5802

Table of Contents

1.0 Introduction 6
2.0 Pre-Test Planning 8
2.1 Test Requirements 8
2.3 Pre-Test Analysis 9
3.0 Test Description 13
3.1 Test Article 13
3.2 Test Instrumentation 15
3.3 Excitation Systems 19
3.4 Data Acquisition System 21
4.0 Stack 1 Test Operation and Data Analysis 22
4.1 Summary of Tests 22
4.2 Random Data Analysis 30
4.3 Sine Sweep Data Analysis 36
4.4 Impact Data Analysis 38
5.0 Experimental Modal Analysis Results 42
6.0 Summary 43
References: 44
Appendix A: Acronyms and Abbreviations 46
Appendix B: Equipment List 48
Appendix C: Instrumentation Setup and Channel Mapping 51
Appendix D: Data Acquisition Log 59
Appendix E: Test Mode Shapes 62

Abstract

Ares I-X was the first flight test vehicle used in the development of NASA's Ares I crew launch vehicle. The Ares I-X used a 4-segment reusable solid rocket booster from the Space Shuttle heritage with mass simulators for the 5th segment, upper stage, crew module and launch abort system. Three modal tests were defined to verify the dynamic finite element model of the Ares I-X flight test vehicle. Test configurations included two partial stacks and the full Ares I-X flight test vehicle on the Mobile Launcher Platform. This report focuses on the second modal test that was performed on the middle section of the vehicle referred to as Stack 1, which consisted of the subassembly from the 5th segment simulator through the interstage. This report describes the test requirements, constraints, pre-test analysis, test operations and data analysis for the Ares I-X Stack 1 modal test.

1.0 Introduction

The 327 foot 1.8 million-pound Ares I-X launch vehicle [1] is shown in Figure 1. Ares I-X consists of a 4-segment reusable solid rocket motor from the Space Shuttle heritage with mass simulators for the 5th segment, upper stage, crew module (CM) and launch abort system (LAS). Ares I-X was successfully launched on October 28, 2009. This was the first flight test for NASA's Ares I crew launch vehicle. Flight test data will provide important information on ascent loads, vehicle control, separation, and first stage reentry dynamics.

As part of hardware verification for Ares I-X, a series of modal tests were designed to verify the dynamic finite element model (FEM) used in loads assessments and flight control evaluations. The first three free-free bending mode pairs were defined as the target modes for the modal test based on the flight control requirements. Since a test of the free-free vehicle configuration was not practical within the projects constraints, calibration of the FEM was done using modal test data for three configurations in the nominal KSC integration flow. The first of these modal tests was performed in May 2009 on the Stack 5 subassembly [2], which included the topmost hardware from the Spacecraft Adapter Simulator to the Launch Abort System Simulator as shown in Figure 2. The second test was performed in July 2009 on the Stack 1 hardware, which included the center section from the 5th Segment Simulator through the Interstage. Finally, the fully integrated Ares I-X flight test vehicle (FTV) mounted to the Mobile Launcher Platform (MLP) was tested in August 2009 [3].

This report focuses on the Stack 1 modal test. The requirements are derived from the free-free bending target modes of the FTV [4]. Based on these requirements, FEM pre-test analysis is used to define the response transducer and shaker locations. Project constraints on instrumentation numbers and vehicle accessibility are also discussed as part of the transducer/shaker placement studies. Schedule constraints required that the team conduct the tests and verify the sufficiency of the data in a short three-day test period. Details of the modal test planning, setup, operation, and results are described. Comparisons between pre-test predictions and test data are provided in Horta [5].

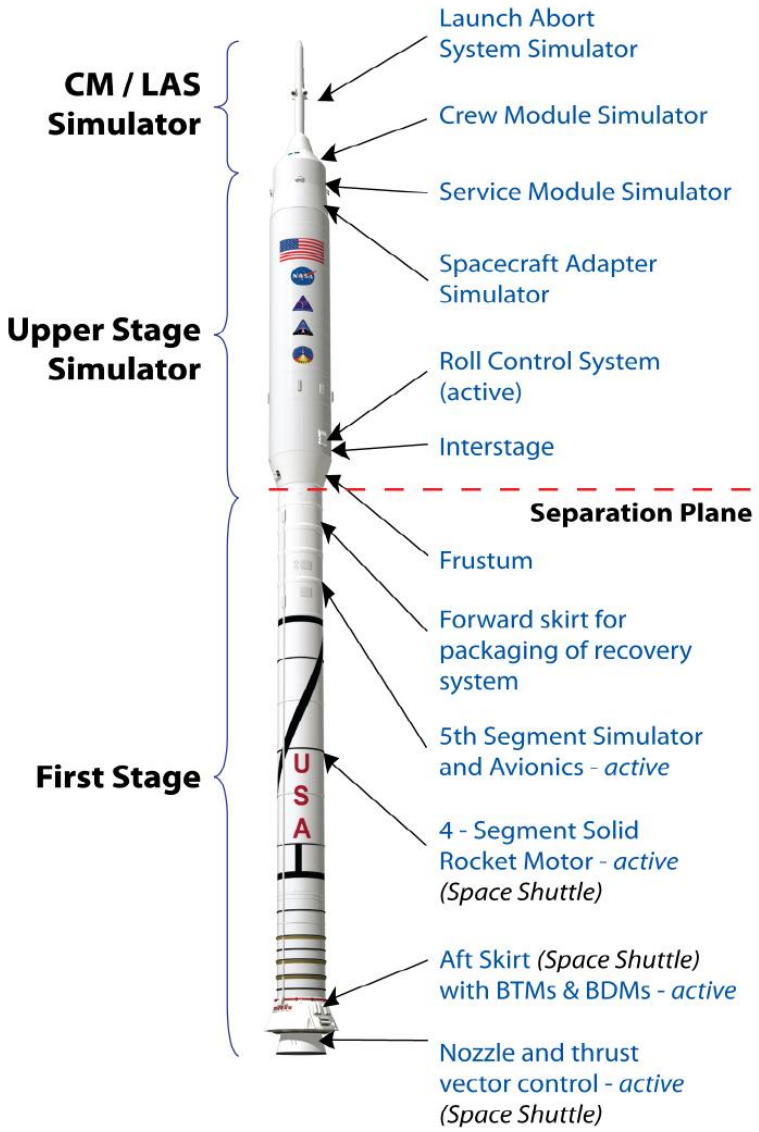

Figure 1. Ares I-X Flight Test Vehicle [1]

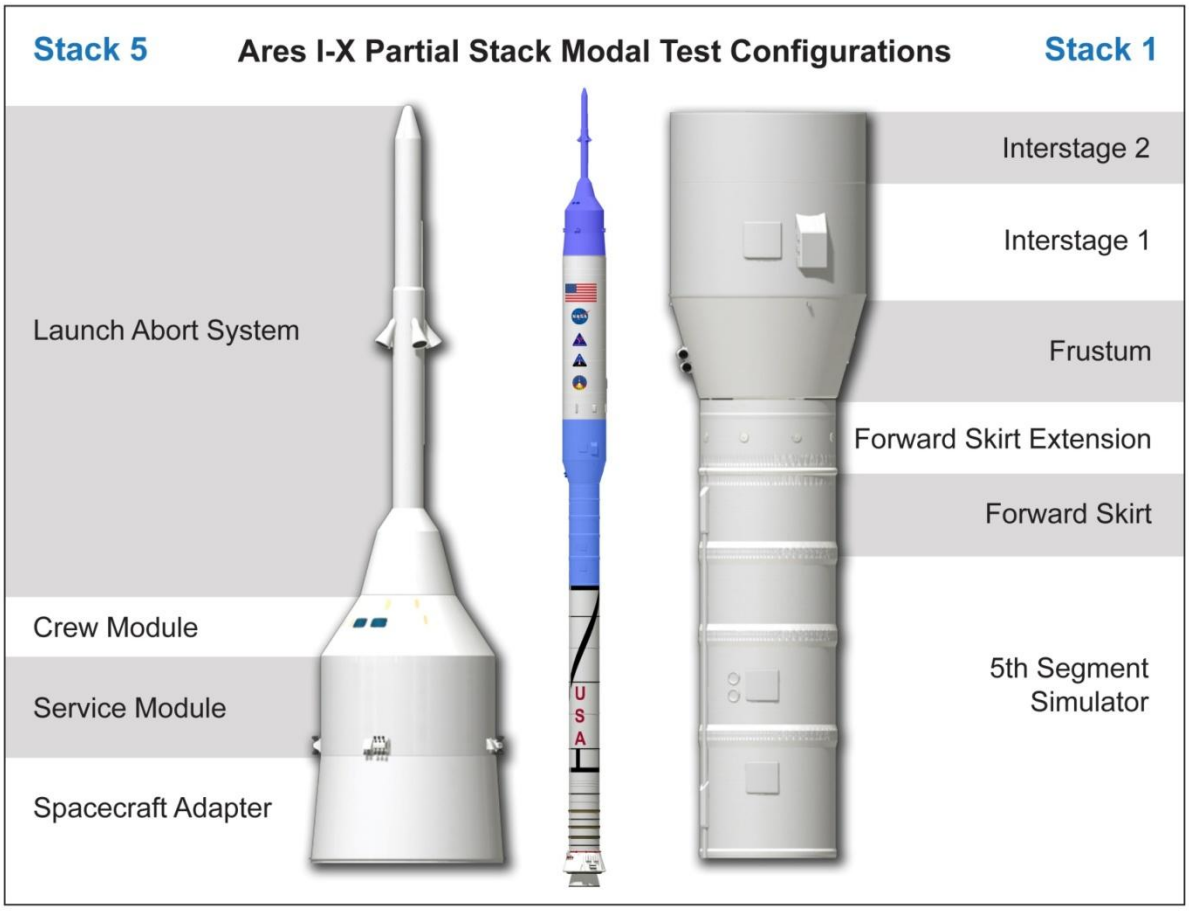

Figure 2. Ares I-X Subassembly Modal Test Configurations

2.0 Pre-Test Planning

2.1 Test Requirements

The Stack 1 modal test was meant to provide an early assessment of FEM adequacy for the subassembly. The project emphasized minimal instrumentation to characterize the bending modes and did not provide hard limits on test/analysis orthogonality metrics. Initially, the goal prior to conducting the pre-test analysis was for approximately 20 sensor locations with biaxial accelerometers for capturing the bending modes. To minimize impact to the program schedule and cost, test durations and configurations were restricted to what was available during the normal vehicle integration flow. Because no special provisions were made for testing, the stack 1 subassembly was tested while shimmed to the floor of the build-up stand in High Bay 4 of the Vehicle Assembly Building (VAB). Testing in the build-up stand of the VAB added two significant constraints to the test setup. First, shaker mounting was restricted to locations accessible from existing facility platforms. Second, the boundary condition

was unknown and would need to be compensated for in the analysis. Early in the planning stage, the test team recognized the risk associated with unknown boundaries and proceeded with an effort to correct for boundary interface compliance [6], and planned for additional measurements across the boundaries. The boundary condition will be further described in the Test Description section.

For flight control, the first three free-free bending mode pairs of the flight test vehicle were critical. Based on these modes, a traceability study [4] was used to define the target modes for the subassembly tests. These target modes will be described in the Pre-Test Analysis section.

2.3 Pre-Test Analysis

The Stack 1 configuration consists of the 5^{th} segment simulator, forward skirt, forward skirt extension, frustum, interstage-1, and interstage-2 as shown in Figure 3. The free end of the 5^{th} segment simulator was shimmed at 12 locations to the buildup stand supports. Additional photographs of the interface will be provided in the Test Description section. For the pre-test analysis, the boundary interface was modeled with springs having a nominal stiffness of $1X10^7$ lb/in at the shim locations. Instrumentation across the boundary was planned to aide in assessing the true interface compliance. Table 1 shows the FEM pretest predictions with the target modes highlighted. The corresponding mode shapes are shown in Figure 4.

Based on these target modes, the effective independence technique [7] along with engineering judgment was used to determine the sensor and shaker locations. The resulting measurement locations are shown on Figure 5. Figure 5 also shows the two shaker locations that were selected based on the constraint of utilizing existing facility platforms for shaker mounting. The 59574 degree of freedom (DOF) FEM was reduced to an 88 DOF test model. The corresponding cross-orthogonality between the reduced model (corresponding to the test instrumentation set) and the full model is used to assess the adequacy of the test instrumentation set as shown in Figure 6. The correlation for the first six modes is consistent with goals of having >0.9 on the diagonal and <0.1 on the off-diagonal terms. This implies that the test instrumentation set is suitable for capturing the first six modes based on the cross-orthogonality metric. The modes with bending (1, 2, 6, 7, and 8) are of primary interest for traceability to the flight test vehicle configuration [4]. Although it is anticipated that modes 7 and 8 will not meet cross-orthogonality goals, qualitative comparisons of mode shapes and frequency response function data will be used to evaluate these modes. This was due to the use of minimal instrumentation and a late update to the FEM after instrumentation installation had begun. Adequate time prior to testing was not available to reassess the instrumentation placement due to the FEM changes. The free-edge at the top of interstage-2 also resulted in significant shell motion (see Figure 4) making it difficult to obtain adequate spatial resolution with the limited instrumentation.

Figure 3. Stack 1 test configuration

Table 1 Pre-Test Analysis Modes for Stack 1

Mode No.	Frequency (Hz)	Mode Description
1	4.07	Stack 1st Bending
2	4.14	Stack 1st Bending
3	16.2	Interstage 2N shell mode
4	16.7	Interstage 2N shell mode
5	17.3	Torsion
6	22.0	Interstage 3N shell mode, coupled with stack 2nd Bending
7	22.7	Interstage 3N shell mode, coupled with stack 2nd Bending
8	23.3	Interstage 3N shell mode, coupled with stack 2nd Bending

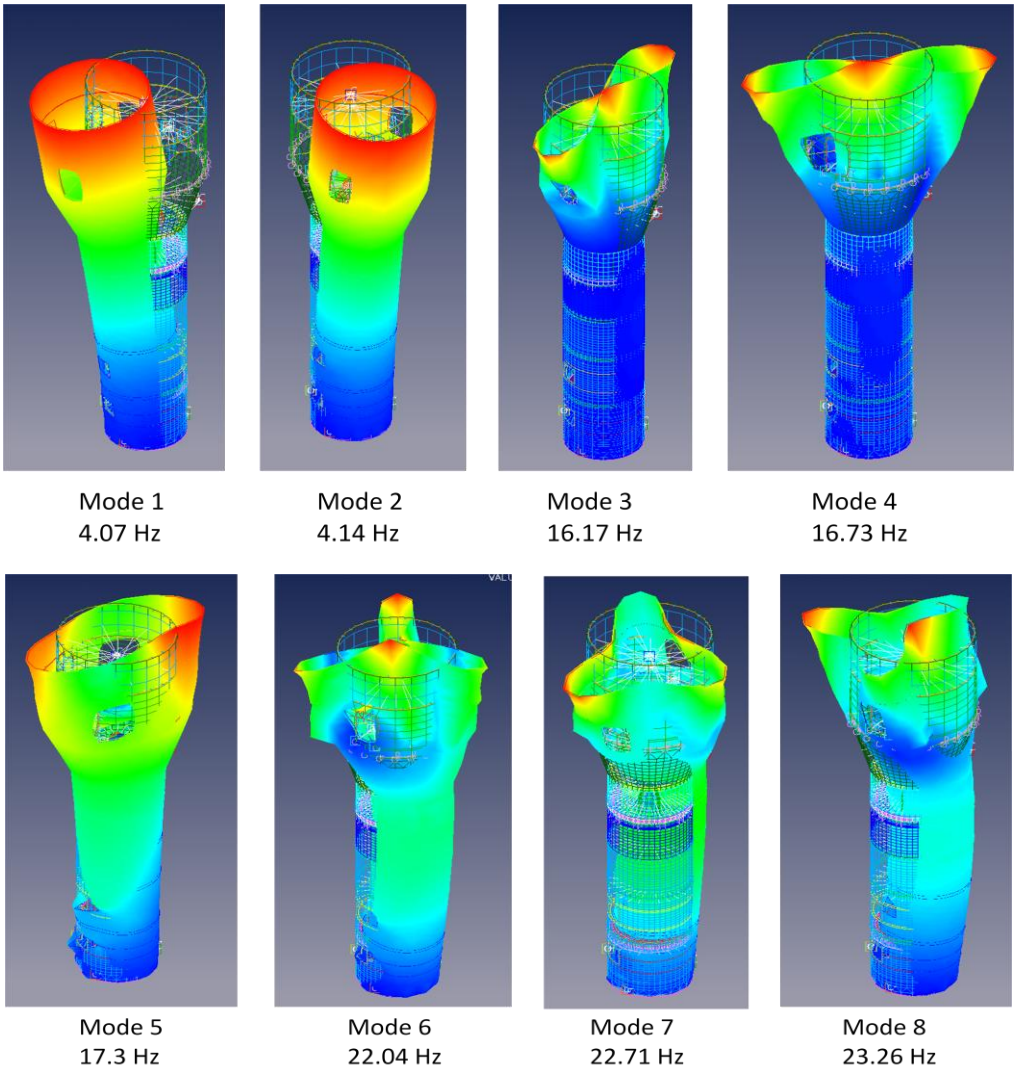

Figure 4. FEM Pre-Test Analysis Mode Shapes for Stack 1

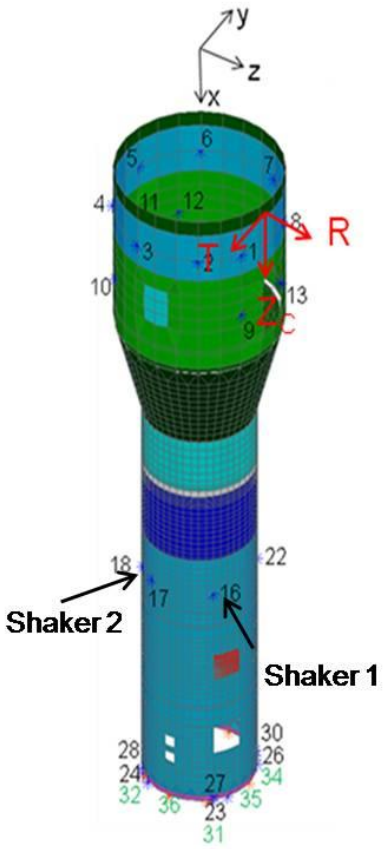

Figure 5. Stack 1 sensor/shaker locations with cylindrical coordinate system in red

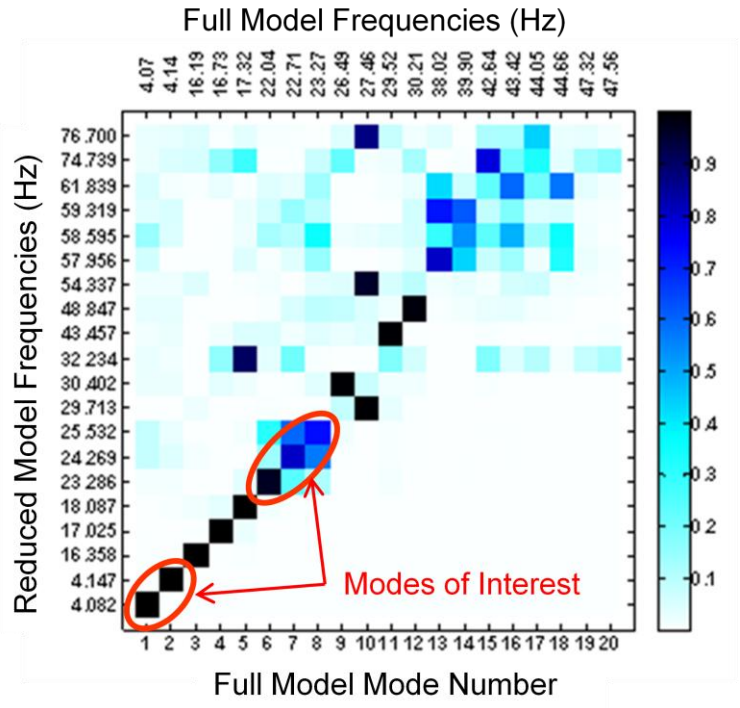

Figure 6. Stack 1 cross-orthogonality

3.0 Test Description

3.1 Test Article

Testing of the 71-foot tall and approximately 150-thousand pound Stack 1 configuration was performed in the build-up stand of High Bay 4 in the VAB as shown in Figure 7. The clevis joint at the free-end of the 5th segment was shimmed at twelve locations to the VAB build-up stand support as shown in Figure 8. This complicated boundary condition has the shims (shown in red) resting on pads that are attached to an I-beam structure (shown in blue) that is in turn resting on concrete piers (shown in green) built into the VAB floor. As a reference, shim 4 aligns with the 90-degree orientation of the flight test vehicle coordinate system. Prior to initiating the assembly of Stack 1, the twelve shims were leveled to within 1/16-inch. When only the 5th segment was installed, five of the shims (locations 2, 5, 6, 8, and 11) could be moved by hand indicating no contact at these locations. The gaps were measured and documented in Figure 8. After the addition of the frustum and interstage components, there was contact at all twelve of the shim locations. As shown in figures 9 and 10, several sets of accelerometers were placed across the boundary in an effort to characterize the boundary condition.

Figure 7. Stack 1 modal test setup with shaker 2 circled in red

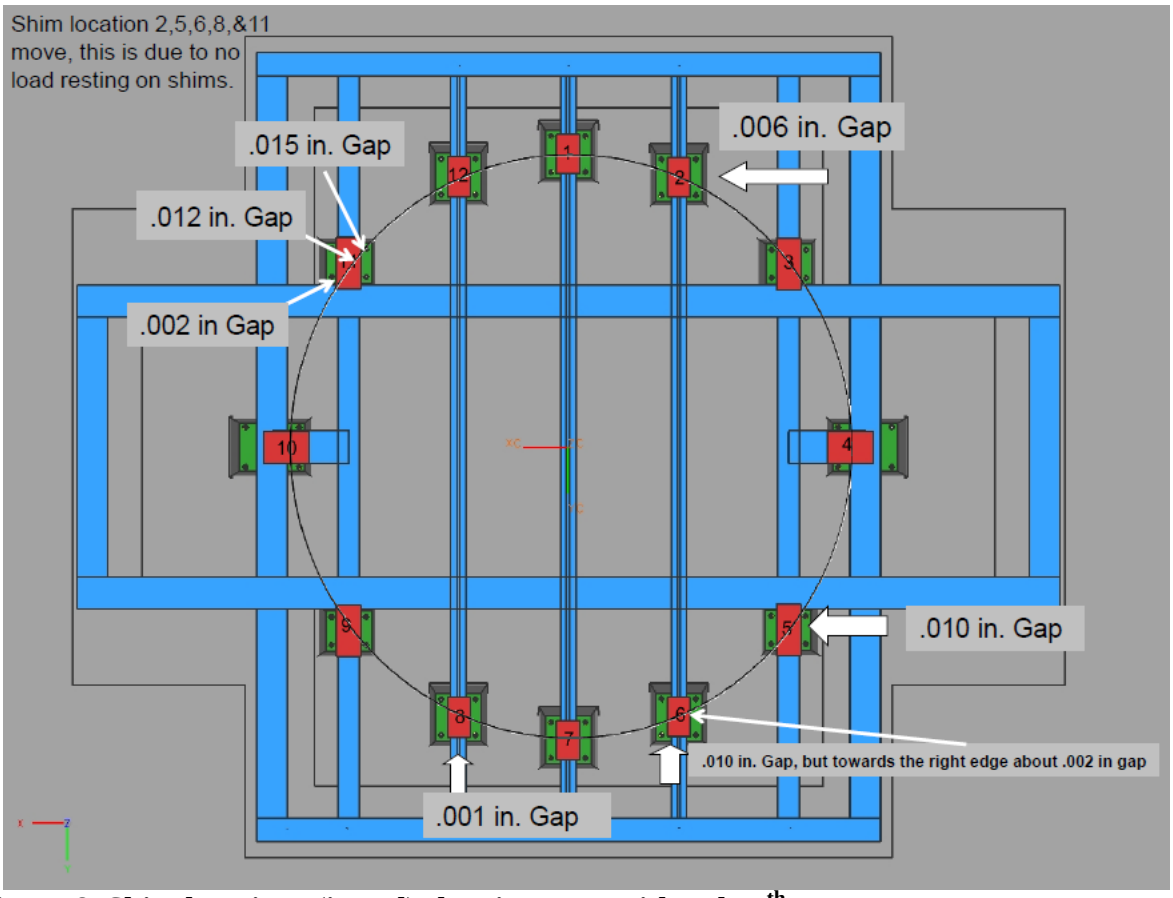

Figure 8. Shim locations (in red) showing gaps with only 5th segment component mounted

Figure 9. Shim plate 4, Accelerometer locations 36

Figure 10. Shim plate 5, Accelerometer locations 24, 28, and 32

3.2 Test Instrumentation

Capacitive accelerometers (PCB Model 3701GFA3G and 3701M 15) were used to measure the dynamic response of the test article. Accelerometer and shaker locations for the Stack 1 configuration are shown in Figure 5 and listed in Table 2. Due to the significant shell type response in the target modes, a cylindrical coordinate system was used for the measurements as shown in Figure 5. Accelerometer installation was performed according to KSC Work Plan FA-GIE-0020, Ares-IX Stack 1 Modal Test-Ground Instrumentation Support. Representative photographs of the accelerometer installations are provided in Figures 9-11. To aide in the investigation of some local response issues for the Flight Termination System (FTS) and First Stage Avionics Module (FSAM), accelerometer locations 46-49 were added after the first test day as shown in Figures 12-14.

Table 2 As-installed Accelerometer Locations

Sensor Location	Radial[1] (in)	Angle[1] (Degrees)	Z[1] (FTV X) (in)	Description	Measurement Axis
1	108.25	30	1859.5	Interstage-2	R, T
2	108.25	60	1858.7	Interstage-2	R, T
3	108.25	105	1860	Interstage-2	R, T
4	108.25	150	1859.2	Interstage-2	R, T
5	108.25	195	1860.5	Interstage-2	R, T
6	108.25	240	1858.2	Interstage-2	R, T
7	108.25	300	1860	Interstage-2	R, T
8	108.25	345	1860.5	Interstage-2	R, T
9	108.25	30	1939.2	Interstage-1	R, T
10	108.25	135	1938.5	Interstage-1	R, T
11	108.25	192	1937.5	Interstage-1	R, T
12	108.25	225	1939.3	Interstage-1	R, T
13	108.25	348	1937.2	Interstage-1	R, T
14	72.79	195	2137	Fwd Skirt Extension	R, T
15	72.79	225	2137	Fwd Skirt Extension	R, T
16	72.79	40	2335.9	5th Segment; Shaker -1	R, T
17	72.79	112.5	2328.3	5th Segment	R, T
18	72.79	140	2336.4	5th Segment; Shaker - 2	R, T
19	72.79	210	2327.7	5th Segment	R, T
20	72.79	232.5	2328.1	5th Segment	R, T
21	72.79	300	2327.7	5th Segment	R, T
22	72.79	330	2327.2	5th Segment	R, T
23	72.79	45	2601.6	5th Segment side of ground interface in-line with 31	R,T,Z
24	72.79	135	2601.6	5th Segment side of ground interface in-line with32	R,Z
25	72.79	225	2601.6	5th Segment side of ground interface in-line with 33	R,T,Z
26	72.79	315	2601.6	5th Segment side of ground interface in-line with 34	R,Z
27	72.79	45	2592.5	5th Segment adapter ring in-line with 23	Z
28	72.79	135	2592.5	5th Segment adapter ring in-line with 24	Z
29	72.79	225	2592.6	5th Segment adapter ring in-line with 25	Z
30	72.79	315	2592.4	5th Segment adapter ring in-line with 26	Z
31	72.79	47	2602.9	Ground shim plate 3	R,T,Z
32	72.79	133	2602.9	Ground shim plate 5	R,Z
33	72.79	228	2602.9	Ground shim plate 9	R,T,Z
34	72.79	313	2602.9	Ground shim plate 11	R,Z
35	72.79	0	2602.9	Ground shim plate 1	Z
36	72.79	90	2602.9	Ground shim plate 4	Z
37	72.79	180	2602.9	Ground shim plate 7	Z
38	72.79	270	2602.9	Ground shim plate 10	Z
39	0	0	1971	IS-1 Platform	R,T,Z
40	54	315	1971	IS-1 Platform	T,Z
41	54.6	45	1971	IS-1 Platform	Z
46	45	150	2480	FSAM 27 Inches from Center Ring-added 7/14/09	-R, T, Z
47	21.25	150	2480	FSAM 3.25 Inches from Center Ring added 7/14/09	-R, T, Z
48	66.79	210	2570	FTS battery added 7/14/09	-R,, -Z
49	69.79	65	2535	FTS added 7/14/09	-R,, -Z

Note[+]: Cylindrical coordinate system referenced to FTV coordinate system: Nominal radius from vehicle centerline; 0 degrees is aligned with +Z-axis and 270 degrees with +Y-axis of FTV coordinate system; Z-axis is aligned with FTV X-axis.

Figure 11. Accelerometer installation on interstage-1 platform

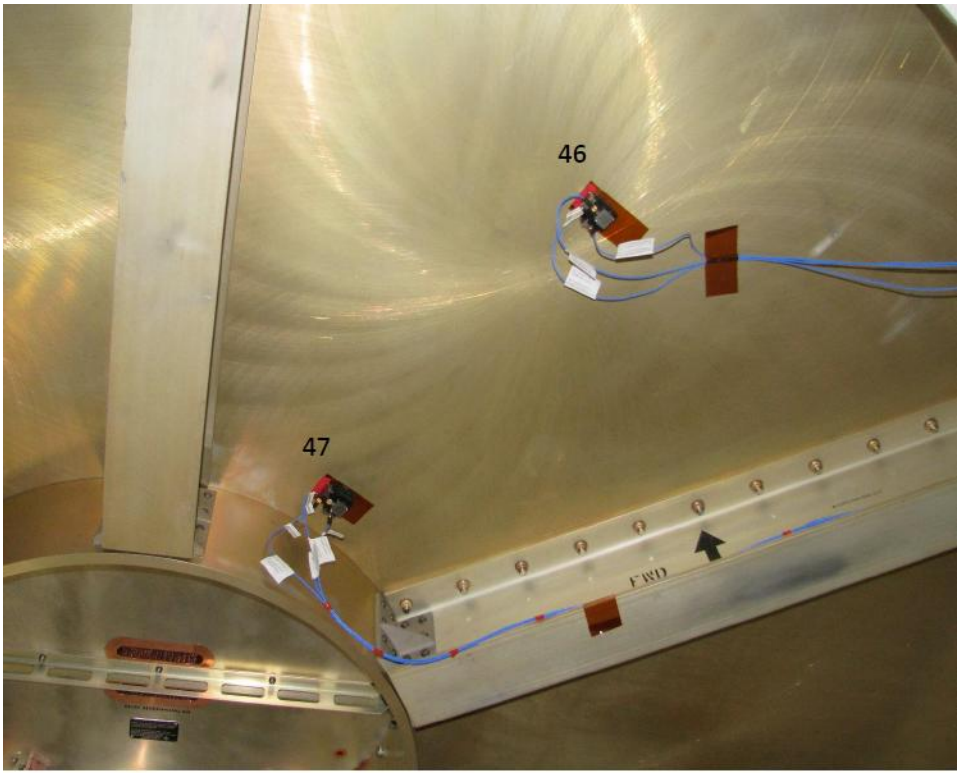

Figure 12. Accelerometer installation on FSAM support plate

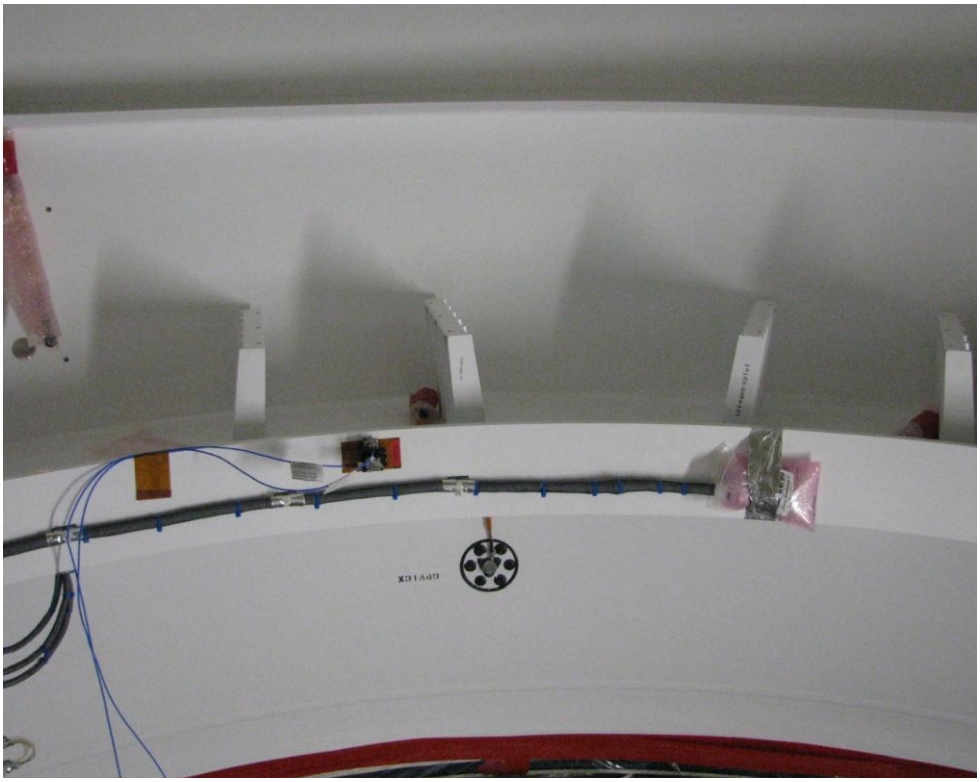

Figure 13. FTS battery mount, accelerometer location 48

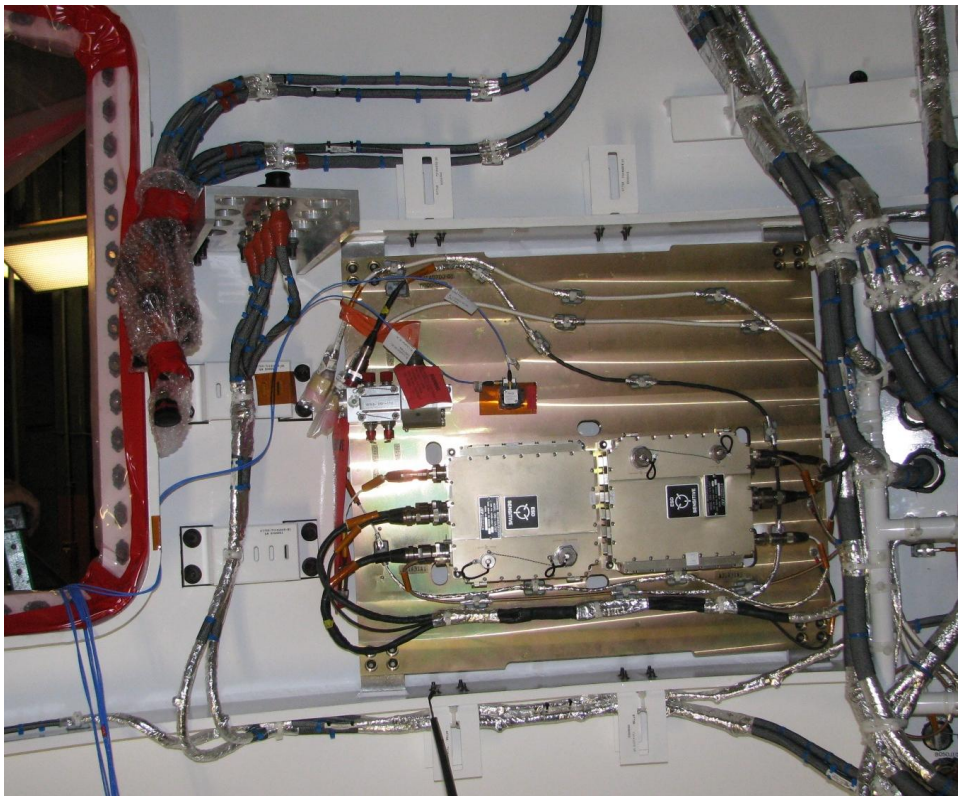

Figure 14. FTS mounting plate, accelerometer location 49

3.3 Excitation Systems

Two MB Dynamics Model 250 electro-dynamic shakers were used to provide excitation to Stack 1 as shown in Figures 15-17. The shakers were attached to a wooden fixture (shown in white) that was bolted to the facility platform using through bolts at two handrail post locations. To impart axial loads while minimizing lateral excitation, each shaker was attached to the test article through a ¼-28 threaded stinger rod. At the point of load application, the stinger rod was threaded into an impedance sensor/adapter plate arrangement as shown in Figure 17. These adapter plates were attached to the test article with dental cement.

The shakers were operated simultaneously for Multiple Input Multiple Output (MIMO) random testing. Several sine sweeps using a single shaker were also performed. The idle shaker was disconnected from the test article during the sine sweeps. In addition to the shaker test, impact tests were performed for several excitation positions with all response data recorded simultaneously. A PCB Piezotronics Model 086B20 hammer was used for impact testing.

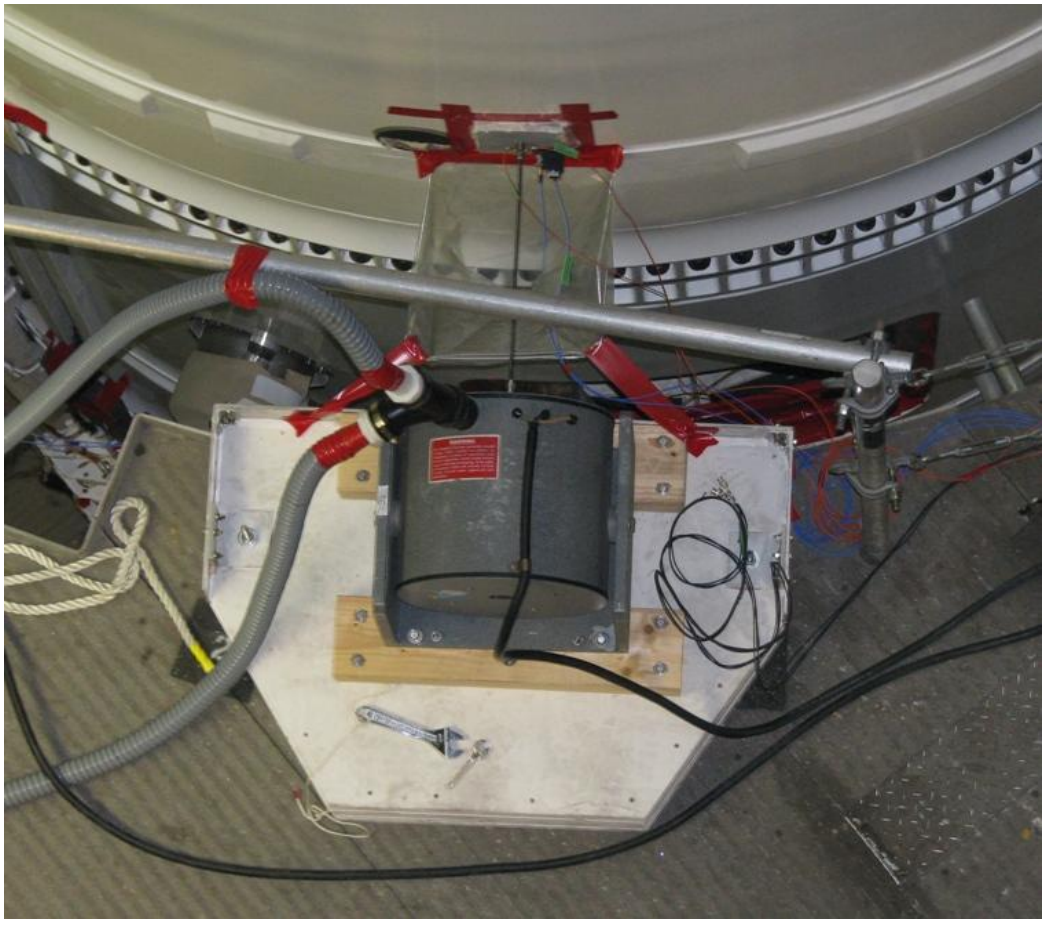

Figure 15. Shaker 1 setup

Figure 16. Shaker 2 setup

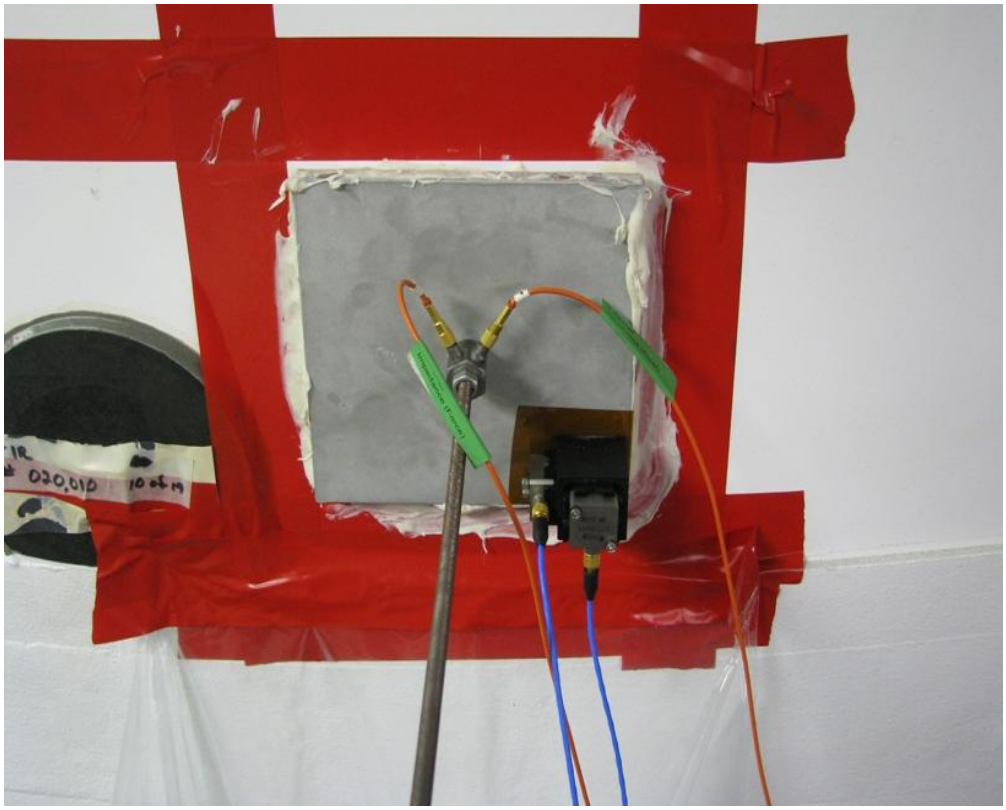

Figure 17. Shaker 1 impedance head and adapter plate setup

3.4 Data Acquisition System

The 112-channel data acquisition system (DAS) consisted of seven 16 channel 24-bit VXI data acquisition cards in a single 13-slot VXI mainframe chassis. Sufficient channels were available to simultaneously sample and record all data. A 16-bit VXI source card in the same chassis provided separate source signals for the excitation system. A Firewire interface card allowed the DAS to be controlled by a data acquisition computer running m+p International's Smart Office Analyzer software. During the test, the software calculated the FRFs from the acceleration and force measurements. For all tests, time and FRF data was stored directly to the computer's hard drive as it was acquired. After each test, the FRFs were exported to a universal file format and supplied to the test team for on-site modal parameter estimation.

A picture of the signal conditioner rack and data acquisition rack as they were configured for the modal test is shown in Figure 18. The signal conditioner rack contained four filters that were used to filter the source signals before they reached the excitation system. The signal conditioner rack also contained the seven signal conditioners used during the test. All of these signal conditioners, plus the filters and the VXI chassis were powered by an Uninterruptible Power Supply (UPS) in the bottom of the signal conditioner rack. A separate UPS located in the bottom of the data acquisition rack was used to power the computer. This isolated the typically noisy computer power supply from the rest of the DAS equipment. For a complete list of the equipment, see Appendix B.

The majority of the signal conditioner channels were routed directly to the data acquisition cards in the VXI chassis using custom-built cables (dark gray cables). BNC cables to patch panels at the top of the data acquisition rack connected the rest of the channels. These patch panels were then connected to the data acquisition cards at the bottom of the rack. For more information on the connections from the instrumentation to the data acquisition system, see the channel mapping in Appendix C.

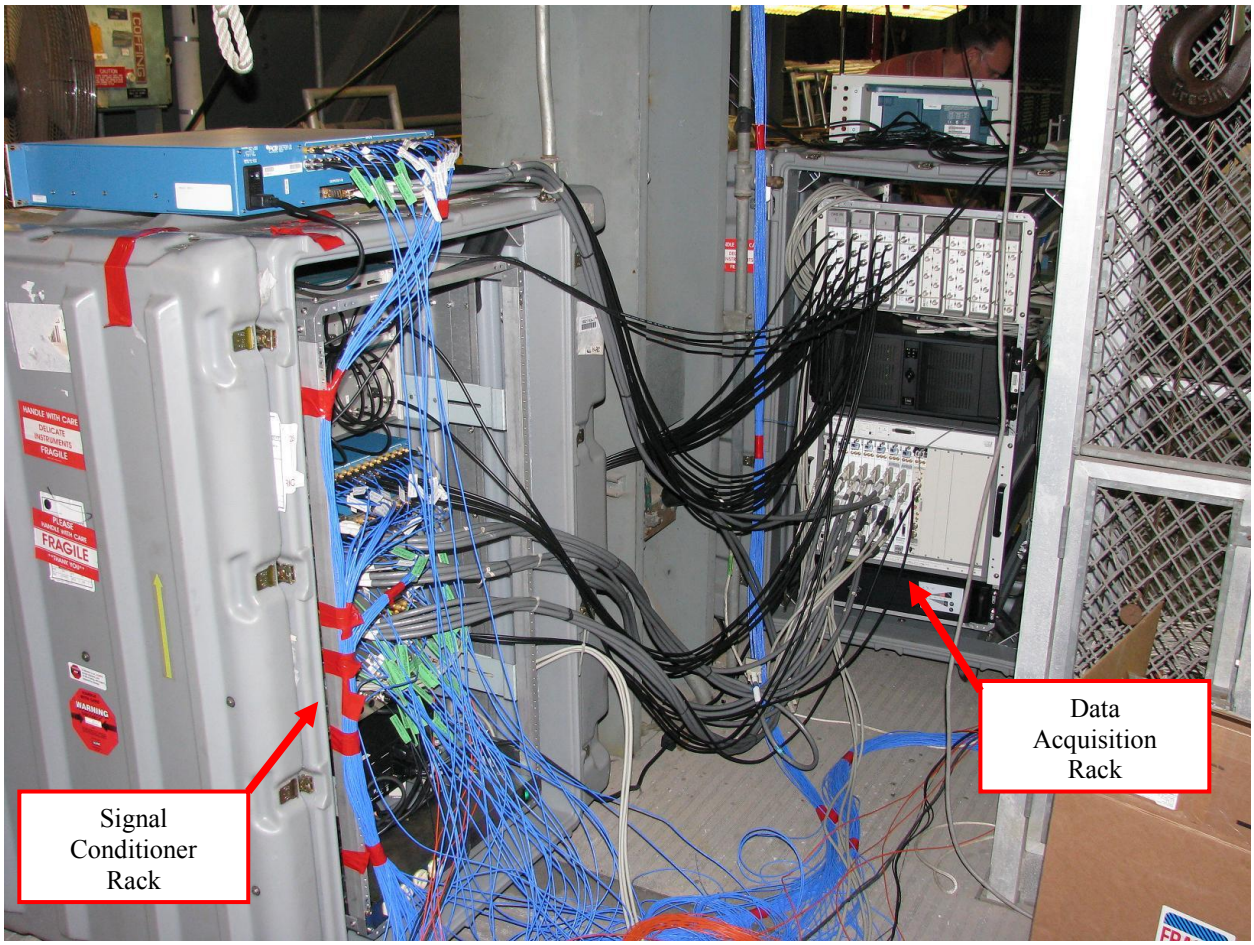

Figure 18. Data acquisition system configuration

4.0 Stack 1 Test Operation and Data Analysis

4.1 Summary of Tests

The modal test was performed by applying a measured excitation force to the test article and measuring the acceleration response at selected locations. The FRFs were calculated as the ratio of the acceleration response to the input force. Modal parameters (natural frequencies, damping factors, and mode shapes) were then estimated from the FRFs. Both the measured FRF data and modal parameter estimates were compared with the pre-test predictions to ensure that sufficient data was acquired to capture the target modes of interest. The primary datasets for modal parameter estimation were FRFs for multi-input random excitation at several force levels. Sine sweeps using a single shaker were used to check for linearity of selected modes with respect to force level. In addition, impact testing was used to provide additional data for model verification.

The test data that was acquired during the Stack 1 modal test is listed in table 3. An accompanying data acquisition log is included in Appendix D. Preliminary testing was performed on July 11 and consisted of Tests SS1-1 through SS1-5. Integration activities were ongoing during these preliminary tests so the data will be influenced by personnel activities.

Evaluation of the preliminary data was used to confirm shaker setup, preferred excitation signal, and accelerometer response characteristics. A review of the preliminary data identified the swapping of data channels 8R and 8T. It was also evident that residual effects from shell modes (>40 Hz) at the shaker input locations were resulting in high modal response estimates at the drive points (see Figure 19). For future tests of cylindrical structures, excitation along a tangential direction should be considered as a means of minimizing this effect. It was also observed that the preliminary mode frequencies were significantly lower than the pre-test predictions, which was attributed to the boundary conditions.

The official test days were July 13 and 15, 2009 and included tests SS1-6 through SS1-17. Several random tests at various force levels, frequency resolutions and excitation bandwidths were evaluated to try to obtain quality frequency response functions. Sine sweep tests at three force levels were used to examine the linearity of the first mode in each axis. In addition, a sine sweep over the 14.1 to 30 Hz range was conducted to try and better resolve the modes in this range. The response of all transducers was also measured for 11 different impact locations. These locations did not correspond to sensor response locations so a brief description of these impact locations is included in Table 4 and shown in Figures 20-28. Locations 52 through 56 were acquired for evaluation of local response of the IS-1 platform, FSAM, and FTS components. Due to available platforms, the shakers were restricted to a relatively low position on the Stack 1 assembly. Therefore, several impact locations (denoted as 50, 51 and 57) were used in an effort to resolve some of the bending/shell modes with significant participation at the top of Stack 1.

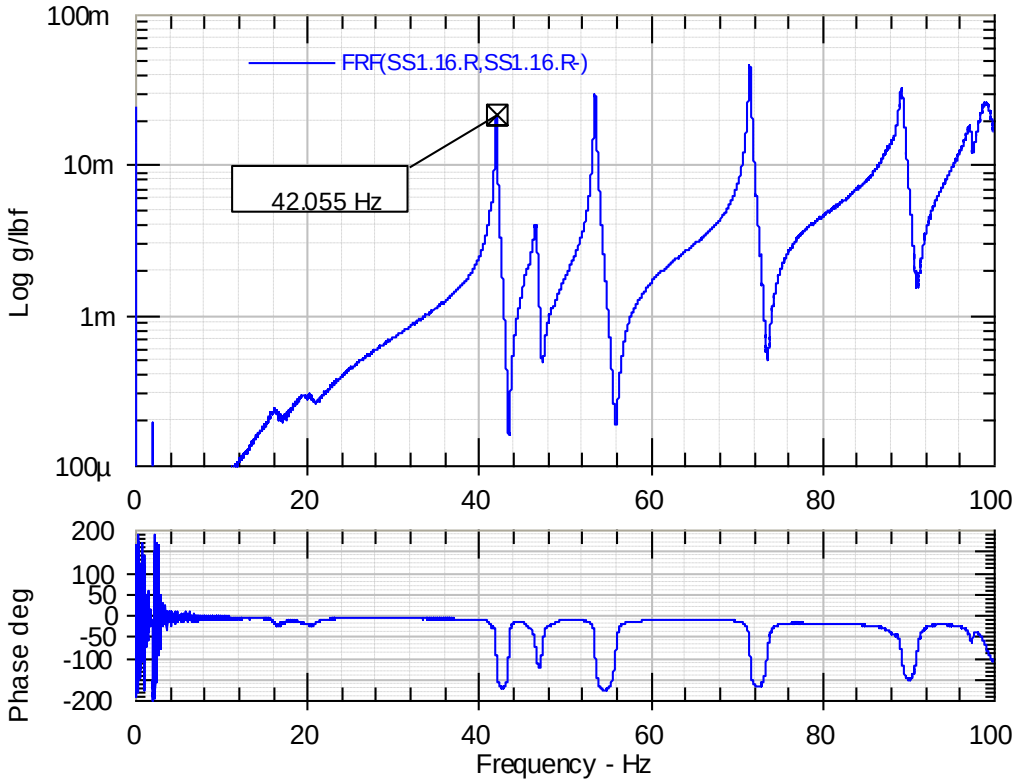

Figure 19. Drive point FRF for test SS1-14 showing dominant out of band modes

Table 3 Super Stack 1 Modal Test Datasets

Test	Run	Type	Level	Direction(s)	Range	Resolution
SS1-1	n/a	Hand Shake Test	n/a	n/a	1 - 50 Hz	0.016 Hz
SS1-2	n/a	Burst Random (50%, 20 avg)	20 lb-rms	16R-, 18R-	1 - 50 Hz	0.016 Hz
SS1-3	n/a	Burst Random (50%, 20 avg)	20 lb-rms	16R-, 18R-	1 - 50 Hz	0.016 Hz
SS1-4	n/a	Random (20 avg)	20 lb-rms	16R-, 18R-	0 - 50 Hz	0.016 Hz
SS1-5	n/a	Impact	n/a	$41X_{FTV}$, 2R	0 - 50 Hz	0.125 Hz
SS1-6	1	Random (16 block, 31 avg)	20 lb-rms	16R-, 18R-	0 - 25 Hz	0.016 Hz
	2					0.0078 Hz
SS1-7	n/a	Random (16 block, 31 avg)	50 lb-rms	16R-, 18R-	0 - 25 Hz	0.016 Hz
SS1-8	n/a	Ambient Noise	n/a	n/a	0 - 25 Hz	0.016 Hz
SS1-9	n/a	Random (16 block, 31 avg)	40 lb-rms	16R-, 18R-	0 - 40 Hz	0.016 Hz
SS1-10	2	Sine Sweep (0.02 Hz/min)	50 lb-pk	16R-	1.91 - 2.13 Hz	n/a
	3		100 lb-pk			
	4		150 lb-pk			
SS1-11	1	Sine Sweep (0.03 Hz/min)	50 lb-pk	18R-	1.54 - 1.72 Hz	n/a
	2		100 lb-pk			
	3		150 lb-pk			
SS1-12	n/a	Random (16 block, 31 avg)	100 lb-rms	16R-, 18R-	0 - 25 Hz	0.0078 Hz
SS1-13	n/a	Ambient Noise	n/a	n/a	0 - 100 Hz	0.0078 Hz
SS1-14	n/a	Random (16 block, 31 avg)	50 lb-rms	16R-, 18R-	0 - 100 Hz	0.0078 Hz
SS1-15	n/a	Random (16 block, 31 avg)	50 lb-rms	16R-, 18R-	0 - 25 Hz	0.0078 Hz
SS1-16	n/a	Impact	n/a	11 locations	0-50/100 Hz	0.125 Hz
SS1-17	1	Sine Sweep (0.75 Hz/min)	50 lb-pk	16R-	14.1 - 30 Hz	n/a
	2		20 lb-pk			

Table 4 Super Stack 1 Impact Locations for Test SS1-16

Point and Direction	Description
50 R-	Top of Frustum at 90° from outside
51 R-	Top of Frustum at 270° from outside
52 X (FTV X)	(See Figure 20) IS-1 platform on outer edge of platform along I-beam at 225° (two people inside but not on platform)
52 T-	(See Figure 21) IS-1 platform on outer edge of platform along I-beam at 225° (two people inside but not on platform)
52 R-	(See Figure 22) IS-1 platform closeout beam at 270° (two people inside but not on platform)
53 X- (FTV X)	(See Figure 23) FSAM base plate at 120°
54 R	(See Figure 24) Below FTS on stiffening ring radial at 65°
54 X (FTV X)	(See Figure 25) Top ring frame about 10” above FTS
55 R-	(See Figure 26) 122” up from shims at ~ FSAM elevation and 150°
56 R-	(See Figure 27) 84” up from shims at ~FTS location and 65°
57 R	(See Figure 28) Top of frustum at 0° (two people inside)

Figure 20. Impact on IS-1 platform on outer edge along I-beam at 225° (52X)

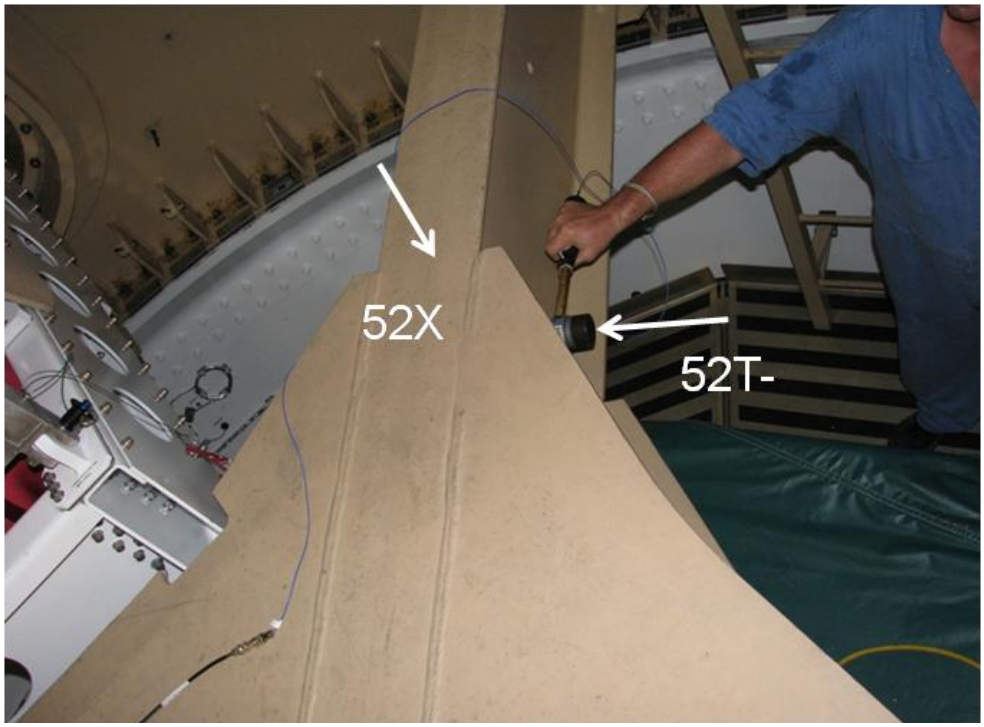

Figure 21. Impact on IS-1 platform on I-beam at 225° (52T-)

Figure 22. Impact radial on closeout beam for IS-1 platform at 270° (52R-)

Figure 23. Impact on FSAM base plate beam at 120° (53X-)

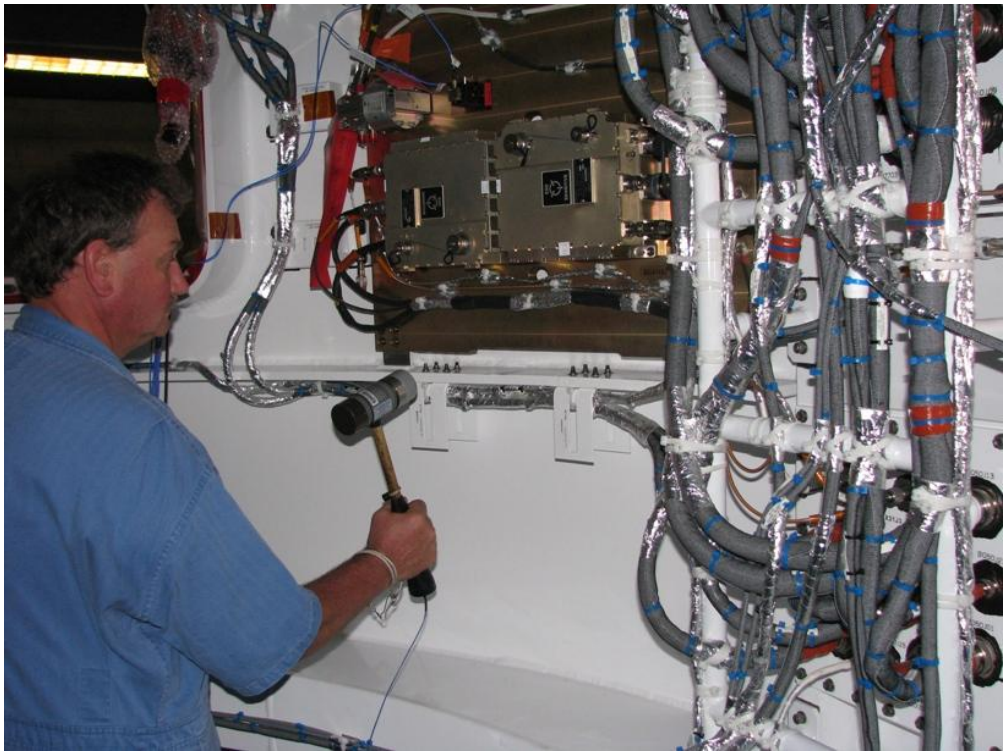

Figure 24. Radial impact on stiffening ring below FTS (54R)

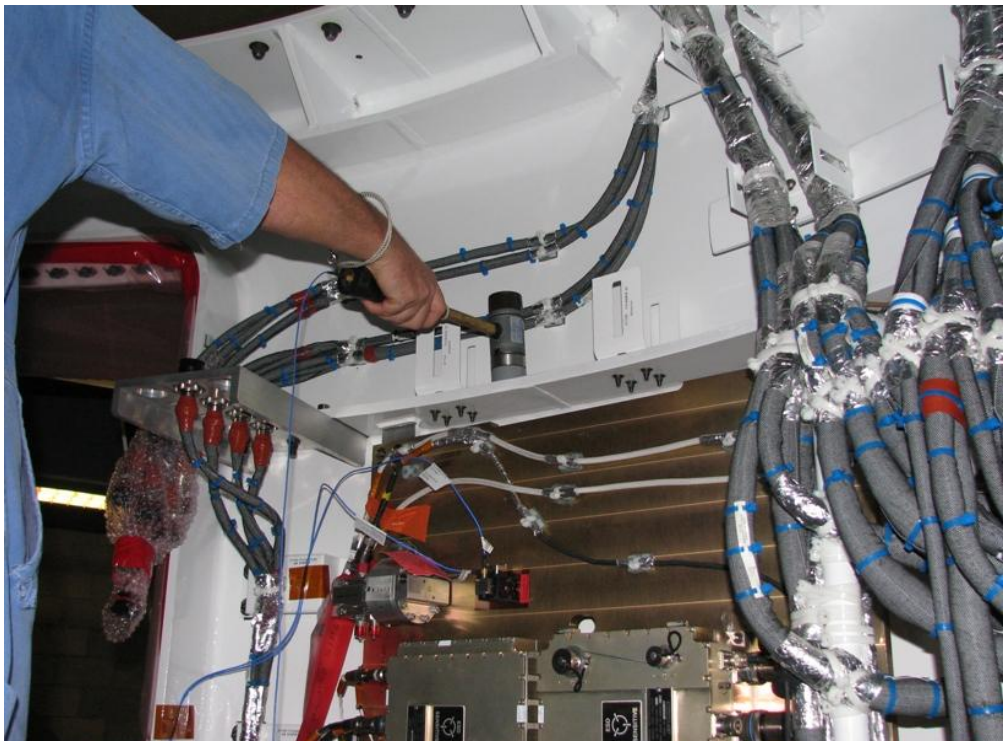

Figure 25. Impact on ring frame above FTS (54X)

Figure 26. Exterior impact 122” up from shims (FSAM elevation) and 150° (55R-)

Figure 27. Exterior impact 84" up from shims at ~FTS location and 65°(56R-)

Figure 28. Impact from inside at top of frustum and 0° (57R)

4.2 Random Data Analysis

The random excitation data sets were the primary data for mode shape estimation and model calibration. In this section, the data quality from these tests is evaluated based on the FRF, coherence, reciprocity, and input force characteristics. Measurement linearity with force amplitude is also examined for the three random input test levels.

Several sets of random data were acquired with various resolutions, frequency ranges and force levels during the first test day. After evaluation of this data, the final sets of random data for modal parameter estimation were acquired with a resolution of 0.0078 Hz. Several of the earlier data sets were acquired using a lower resolution, but these were more difficult to curve fit. Two other data sets used higher sample rates to investigate higher frequency phenomena, but this also spread the force out over a larger frequency range, resulting in less force being concentrated at the target modes.

Sample FRF and coherence data from the 50 lb-rms random test SS1-15 is shown in Figures 29 and 30 below. The blue curves representing the drive point FRFs show the peaks associated with the first bending modes around 2 Hz, but the higher frequency response is dominated by residual effects from shell modes above the frequency range of interest. This dominant high frequency shell mode did not affect any other measurements besides the drive points in the radial direction. FRFs for radial and tangential measurement points near the top of the structure (red and green curves) show the 1st bending modes as well as higher order modes above 10 Hz. The multiple coherence functions (cyan, magenta, and yellow curves) between the response measurements and both input measurements were generally near 1 across the measurement bandwidth, with the exception of a few frequencies where the coherence drops to ~0.6 near the first bending modes and 0.8 at some anti-resonances.

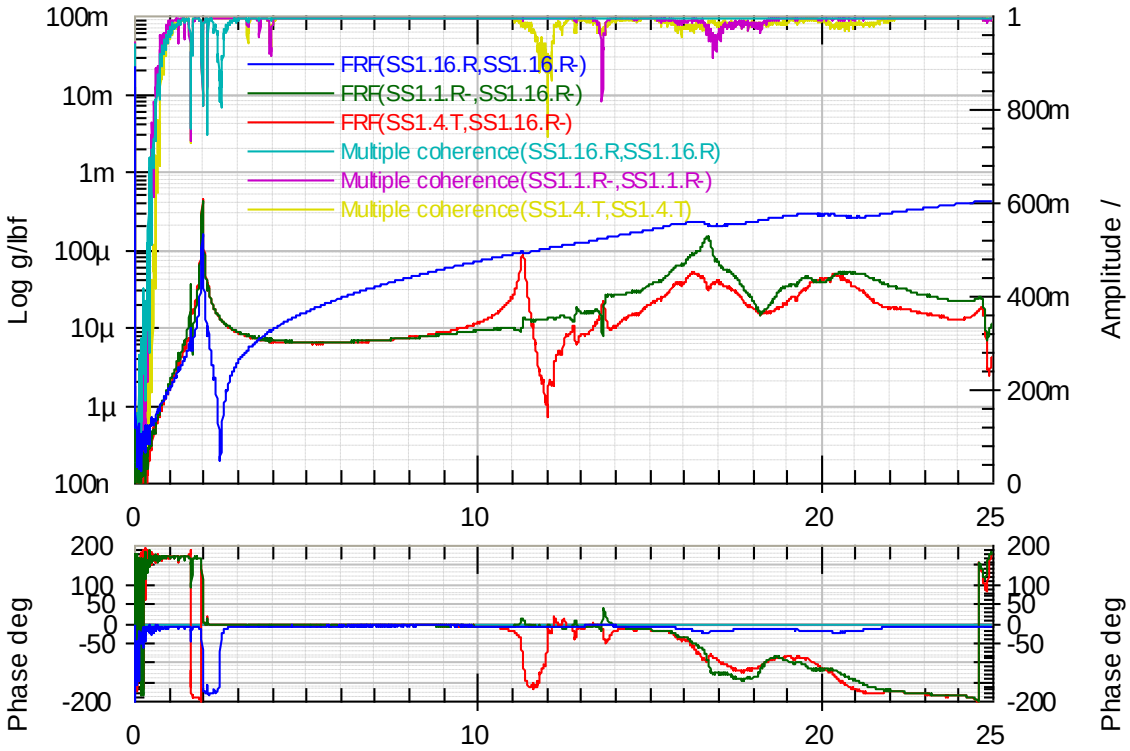

Figure 29. Shaker 1 reference FRFs and coherence from SS1-15 random test

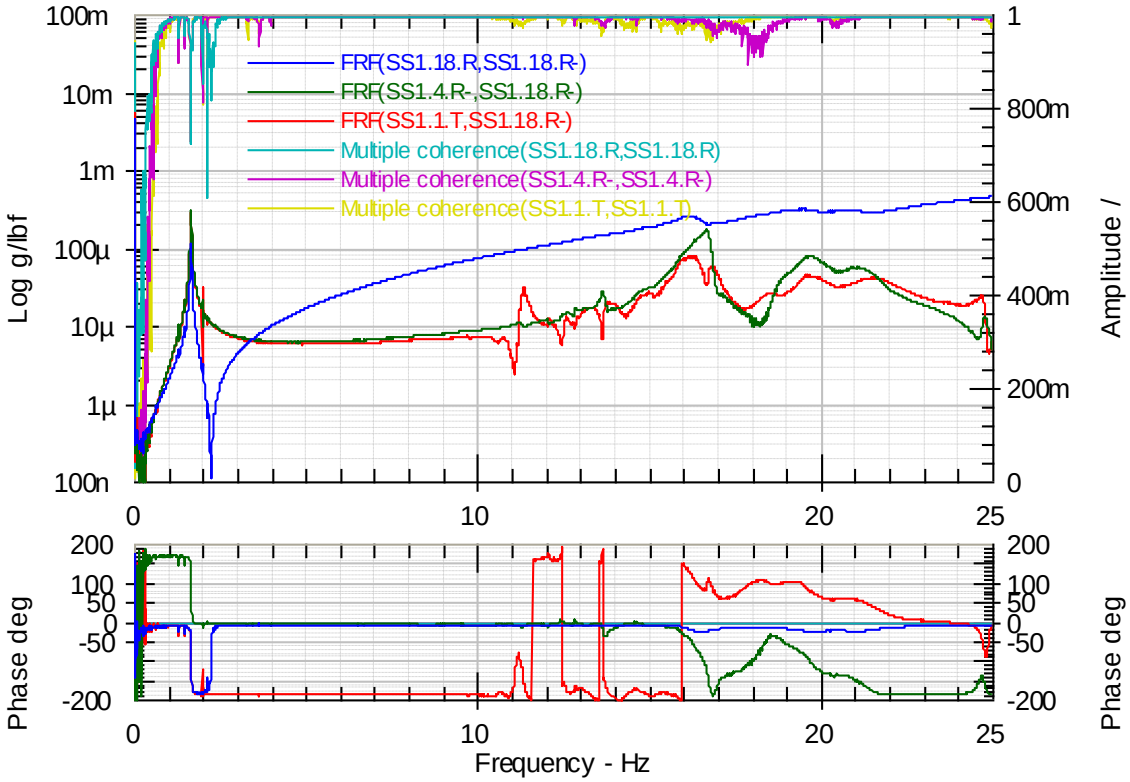

Figure 30. Shaker 2 reference FRFs and coherence from SS1-15 random test

The result of a reciprocity check (FRF of the response acceleration at one shaker location compared to the input force at the other shaker location) from the 50 lb-rms random test SS1-15 is shown in Figure 31. Differences between the two FRFs indicate possible nonlinearities in the 8 to 22 Hz range. Due to noise issues on the impedance head accelerometers, nearby accelerometers located on the shaker adapter plates (see Figure 17) were used for the reciprocity check. Some of the differences between the FRF measurements may be due to the fact that the load cell and drive point accelerometers were not co-located.

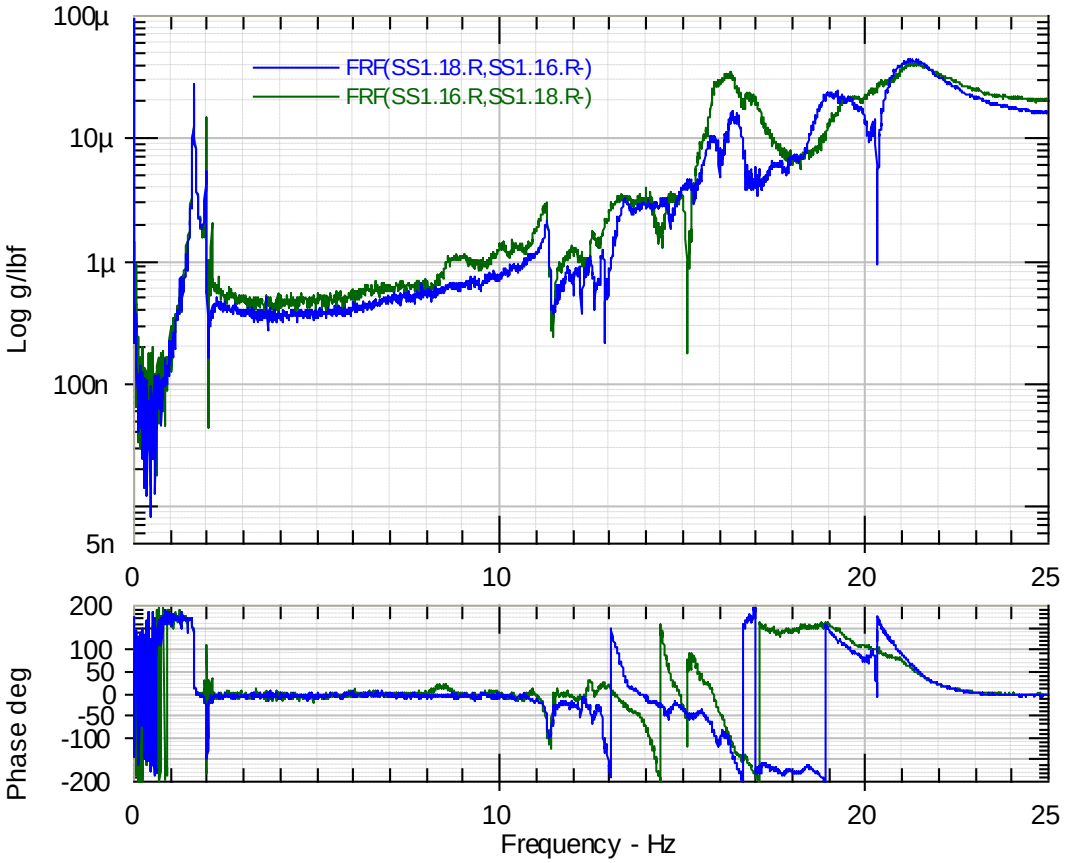

Figure 31. Reciprocity from SS1-15 random test

In order to check that the work platform the shakers were mounted to did not have an effect on the input force, the autospectra of the input forces were checked for significant dips. Figure 32 shows the autospectra for the 50 lb-rms force SS1-15 random test, which did not indicate any significant dips over the frequency range of interest.

Another check on the input forces was performed using principal component analysis. Results of this analysis for the SS1-15 random test are shown in Figure 33. The blue and green curves are the principal input force spectra, and there was not more than a 10 dB drop between the two across the frequency band. This indicates that there is little to no correlation between the input force signals in the bandwidth of interest. This conclusion can also be reached by observing the coherence between the input forces, which was near zero across the frequency band.

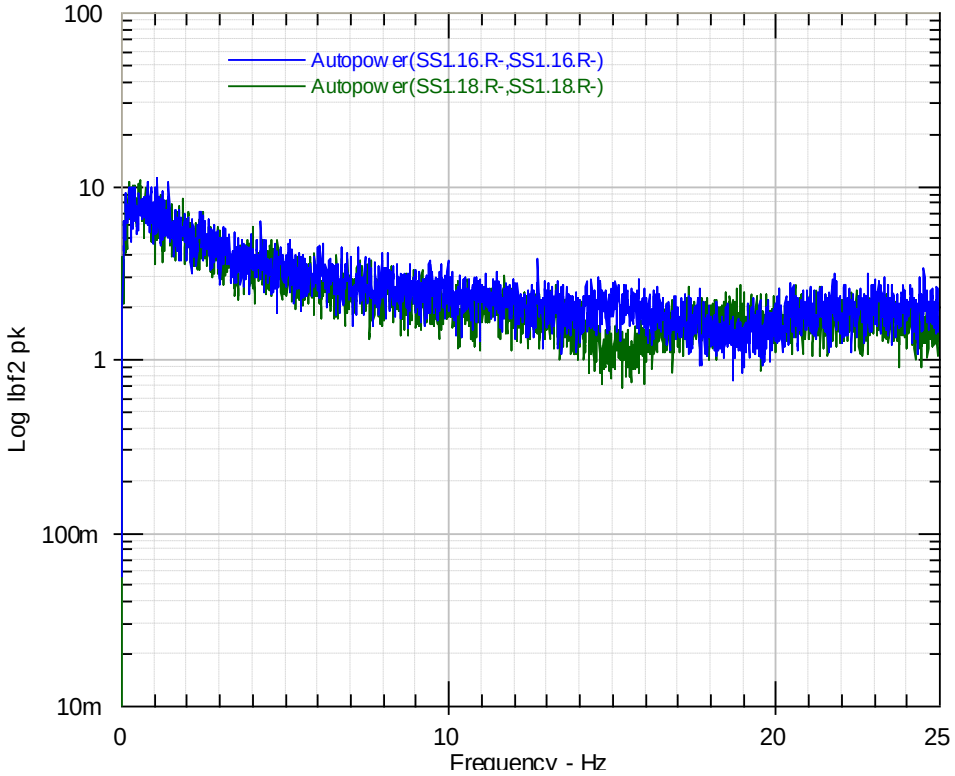

Figure 32. Input autopower from SS1-15 random test

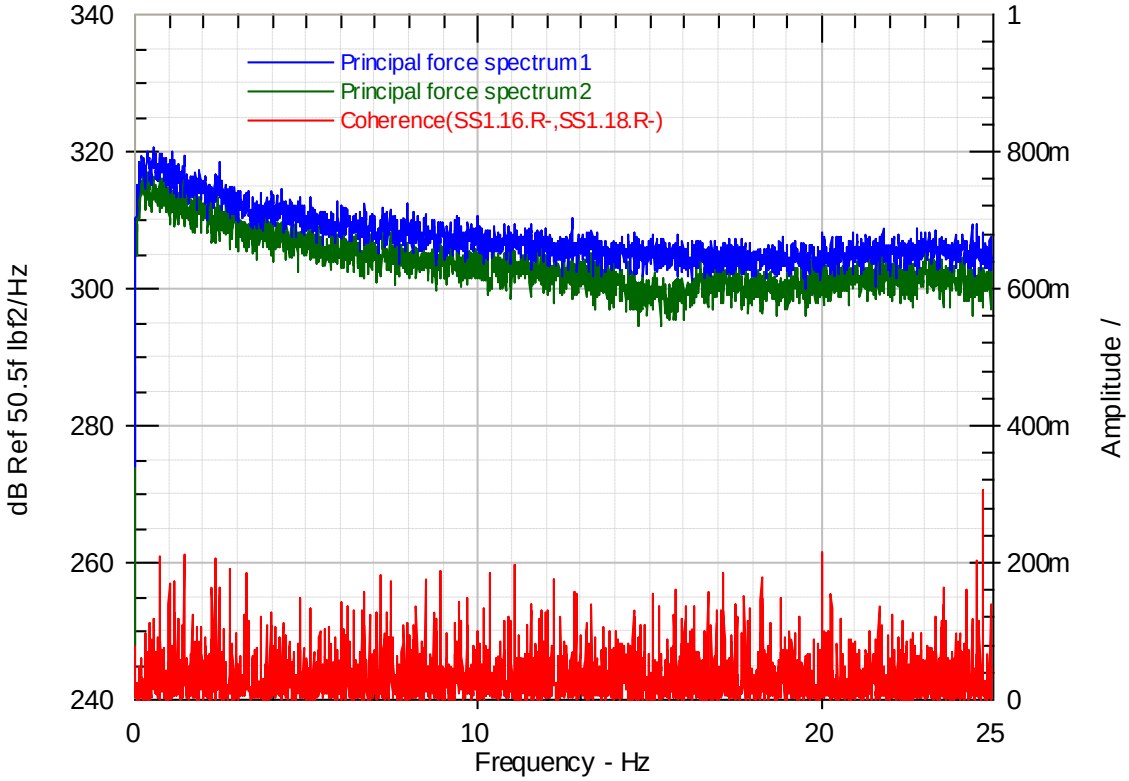

Figure 33. Principal input spectra and coherence from SS1-15 random test

Figures 34-36 show a comparison of the random FRFs for three force levels. As shown in the figures, the Stack 1 subassembly has some change in the FRFs due to force level. This is highlighted in the zoomed areas of Figure 36. Table 5 shows the peak frequencies for the 1st bending modes, which varied by as much as 2.3% from the 20 lb-rms to 100 lb-rms tests. The data indicates some nonlinearity in the structure or boundary conditions for the tested force levels. Because the nature of random excitation is to linearize test results, sine sweep tests were also performed to investigate possible nonlinearities in the test article.

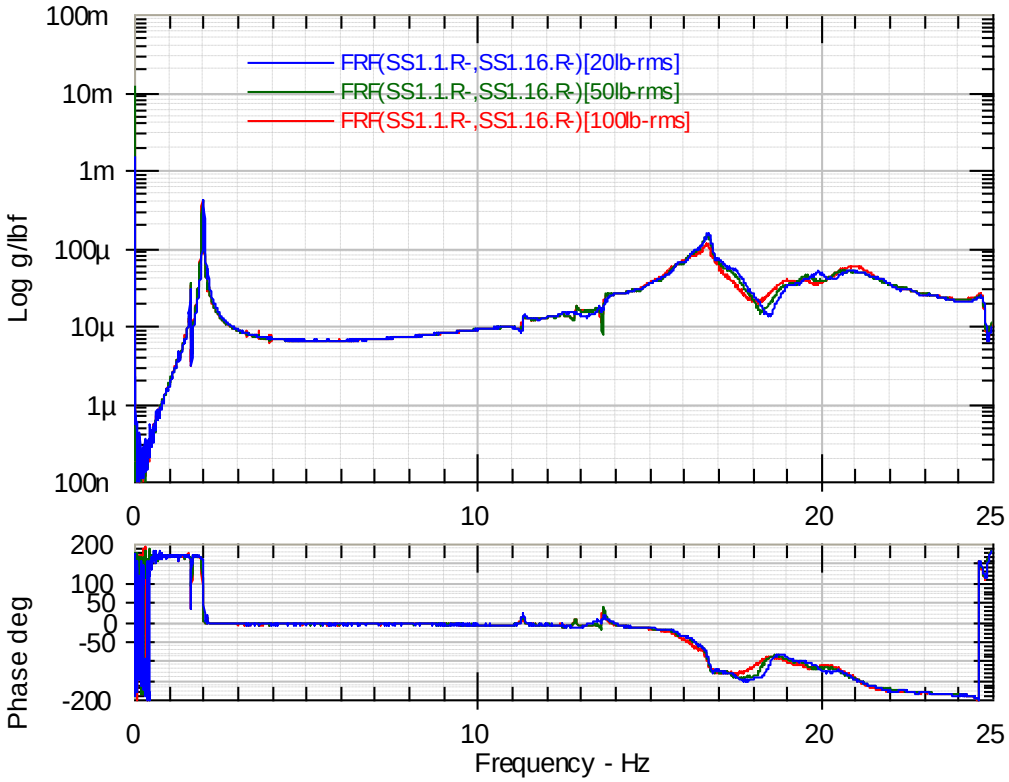

Figure 34. Radial direction FRFs from random tests SS1-6(Run 2), SS1-12, and SS1-15

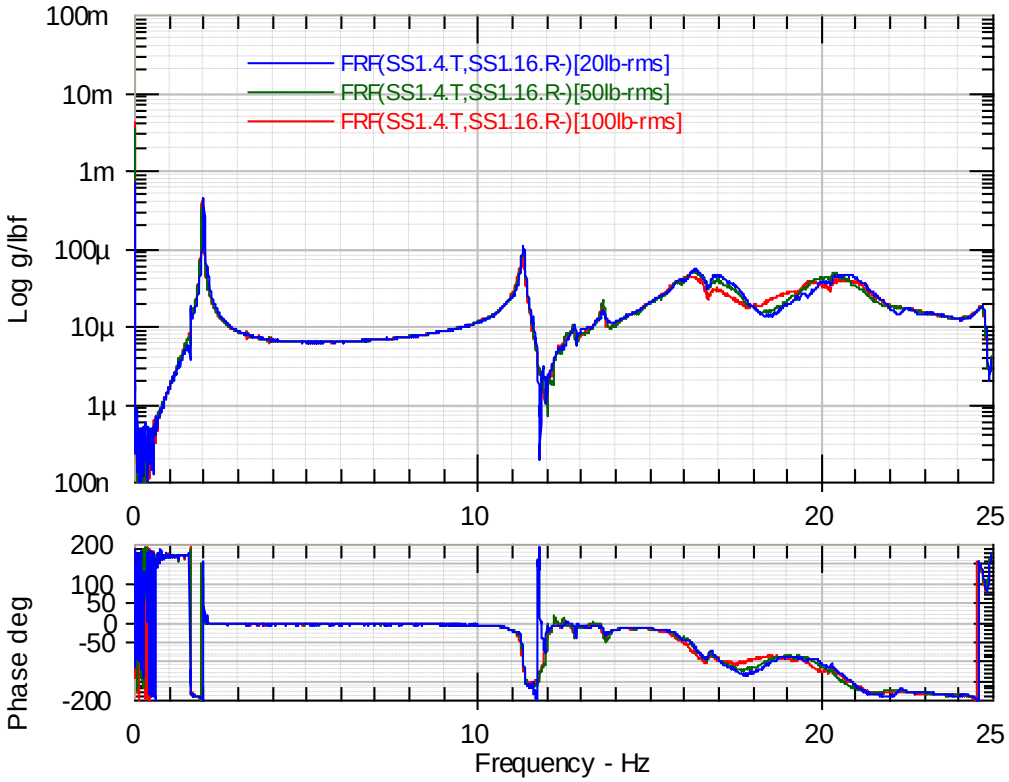

Figure 35. Tangential direction FRFs from random tests SS1-6(Run 2), SS1-12, and SS1-15

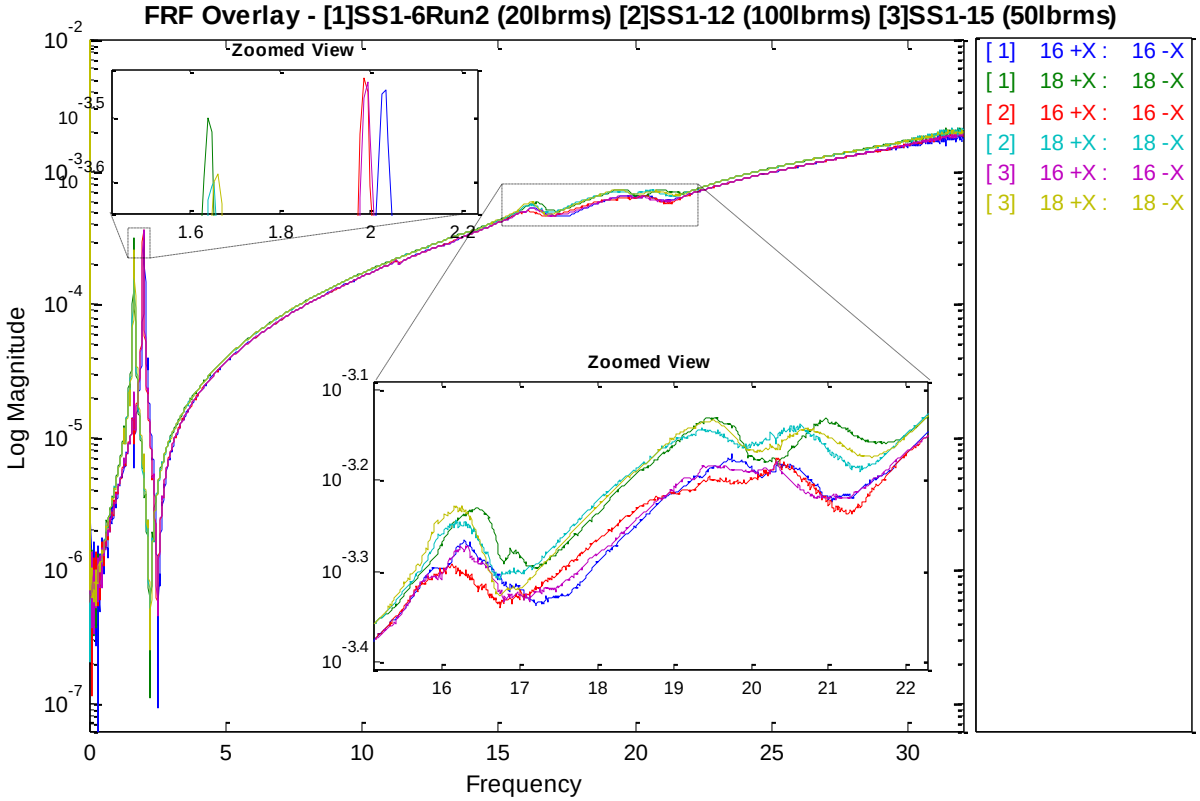

Figure 36. Drive point FRFs from random tests SS1-6(Run 2), SS1-12, and SS1-15

Table 5 Peak Frequency Variation for Random Excitation

Mode	Random 20 lb-rms Peak Frequency (Hz)	Random 100 lb-rms Peak Frequency (Hz)	Percent Difference (%)
1	1.64	1.66	0.96
2	2.03	1.98	-2.31

4.3 Sine Sweep Data Analysis

Sine sweep tests were performed to evaluate the linearity of the response with respect to excitation level. One important parameter for obtaining useful results from a sine sweep is the sweep rate. Sweep rates were selected based on the recommendation by Ewins [8] that the sweep rate must be less than $216(f_n)^2(\zeta_n)^2$ Hz/min. Each mode was swept individually from -6% to 5% of the natural frequency estimated from the curve fit of the random data sets. Some sweeps were stopped before reaching 5% of the natural frequency if the data indicated that the response was less than half of the peak value. This can be seen in Figure 37, where the red curve was a 50 lb-pk sweep across the -6% to 5% frequency range, but the 100 lb-pk green and 150 lb-pk blue curves were stopped earlier. Note that Figures 37 and 38 are the response amplitude in g's versus the sweep frequency. The frequencies at the peak response for each case are listed in Table 6. The peaks in Figure 37 indicate that mode 2 had a 1.9% change in peak frequency for the three-time change in force, which is comparable to the change observed in the random tests. For mode 1, the peak frequency change was more significant for the sine sweeps resulting in a 3.7% difference for the three-time change in force. The reason for the nonlinearity is likely due to the uncertain boundary condition for the Stack 1 test and may not be representative of nonlinearity in the Stack 1 structure itself. However, there is no means to separate the influence of the structure and boundary condition.

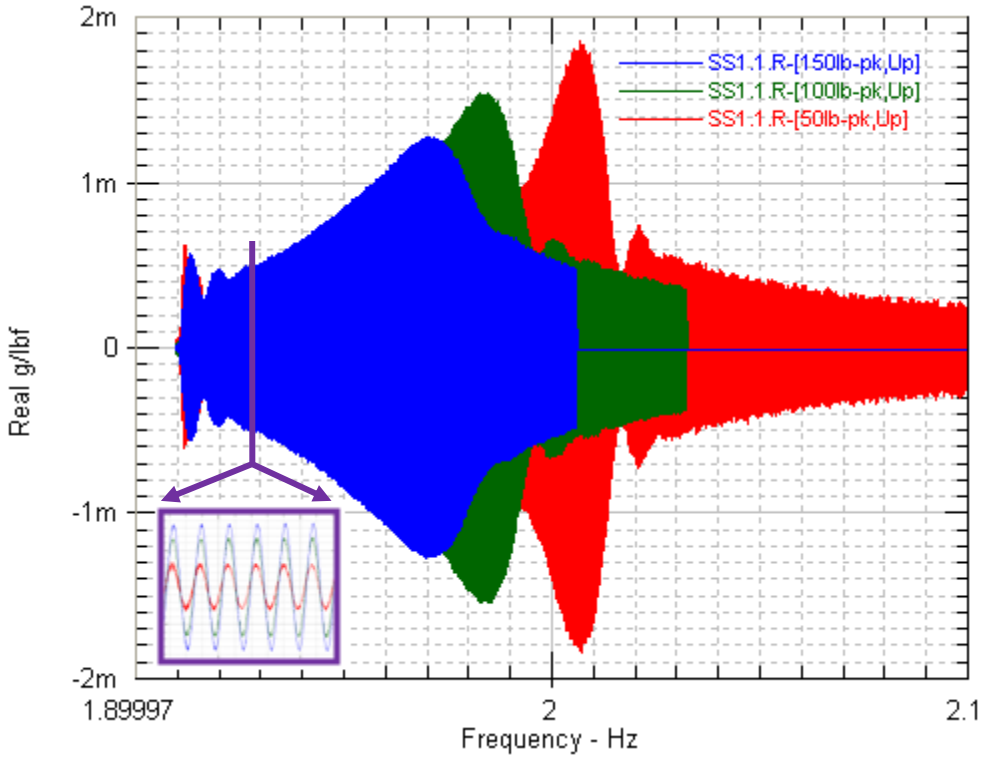

Figure 37. Variation in mode 2 due to varying sine sweep levels (SS1-10)

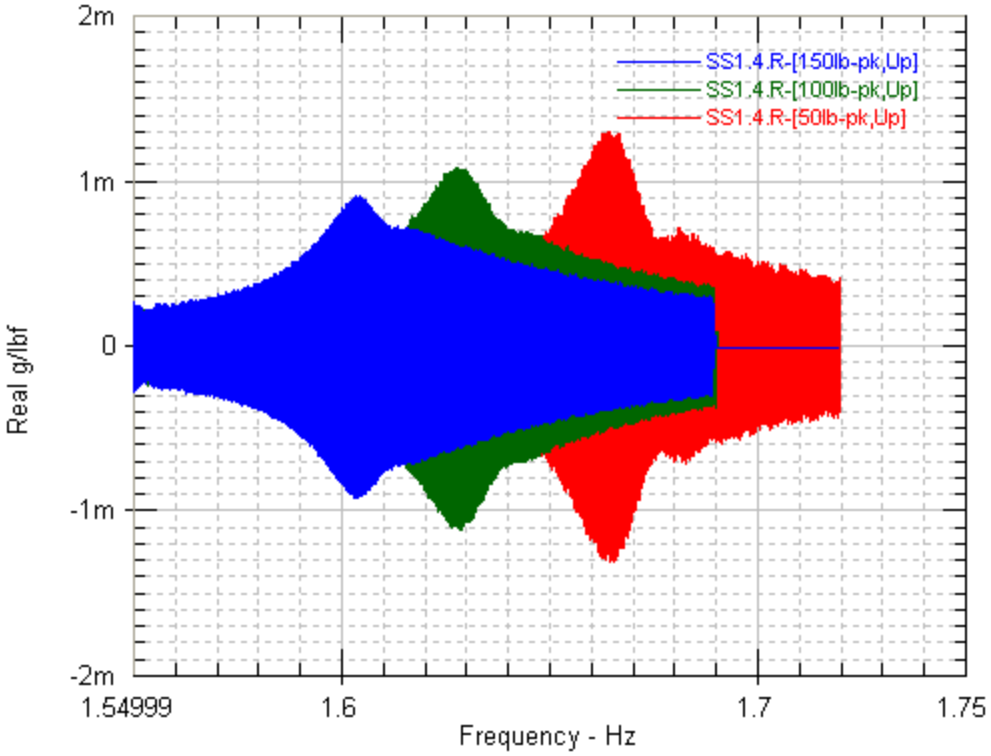

Figure 38. Variation in mode 1 due to varying sine sweep levels (SS1-11)

Table 6 Peak Frequency Variation Due to Sine Sweep Excitation Level

Mode	Sweep Up 50 lb-pk Peak Frequency (Hz)	Sweep Up 100 lb-pk Peak Frequency (Hz)	Sweep Up 150 lb-pk Peak Frequency (Hz)	50 vs. 150 lb-pk Percent Difference (%)
1	1.6649	1.6284	1.6037	-3.68
2	2.0070	1.9850	1.9698	-1.85

4.4 Impact Data Analysis

Impact tests were used during the Stack 1 modal test in order to investigate local modes of individual components and to help resolve some of the bending/shell modes with significant participation at the top of Stack 1. Sampling parameters were a 128 Hz sample rate, 8-second block size, and 5 averages. At some locations, a 256 Hz sample rate was used in order to identify peak responses out to 100 Hz. Chosen locations included an internal platform, the frustum, the FSAM mounting location, and the FTS mounting location as defined in Table 4.

At the request of the project, sensors were added to the FSAM and FTS to evaluate local mode response and the potential for tuning with anticipated launch forcing frequencies. The axial impact response of the FSAM is shown in Figure 39. Natural frequencies at 43.1 and 91.4 Hz correlated well with predictions of FSAM platform modes. For the FTS, radial and axial impacts are shown in Figure 40. Modes to approximately 40 Hz appear to align with global modes of Stack 1 but the dominant frequencies between 79.3 and 104 Hz may be local modes of the FTS mounting plate. This data was provided to the project for further assessment.

To aide in the resolution of the Stack 1 global modal response, several impacts were made on the IS-1 platform and frustum. Figure 41 shows axial impact response of the IS-1 platform, which indicates modal response at 16.6, 38.3 and 45.9 Hz. A global mode of Stack 1 is at 16.6 Hz but the modes at 38.3 and 45.9 Hz appear to be local modes of the platform in the axial direction. Responses from impacts at the frustum are shown in Figure 42. The dominant modal response indicated at 13.6 and 25.6 Hz align with shell modes of Stack 1. A comparison of sample FRFs from the random shaker (Test: SS1-9) and impact tests is provided in Figures 43 and 44. Based on this response comparison, it is evident that the shakers are not positioned well for exciting some of the shell/bending modes that have significant participation at the Interstage level. Therefore, some further clarification of modes may be possible through detailed analysis of the frustum impact data.

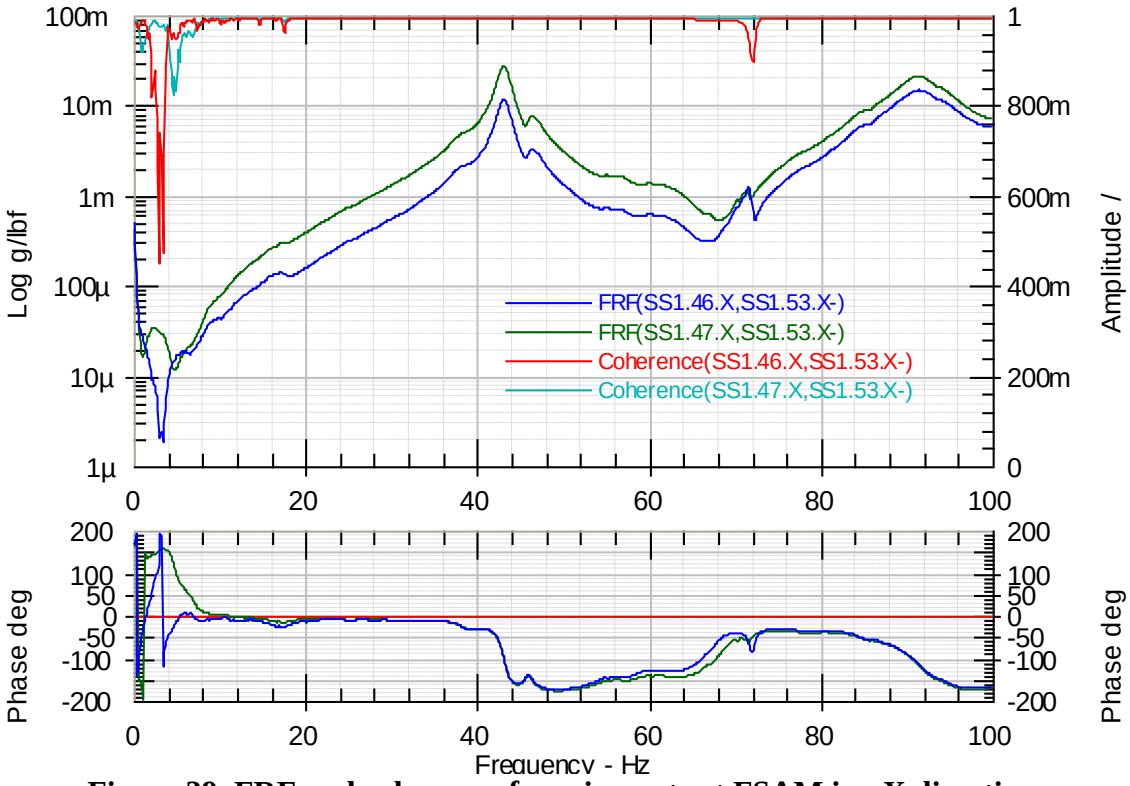

Figure 39. FRF and coherence from impacts at FSAM in –X direction

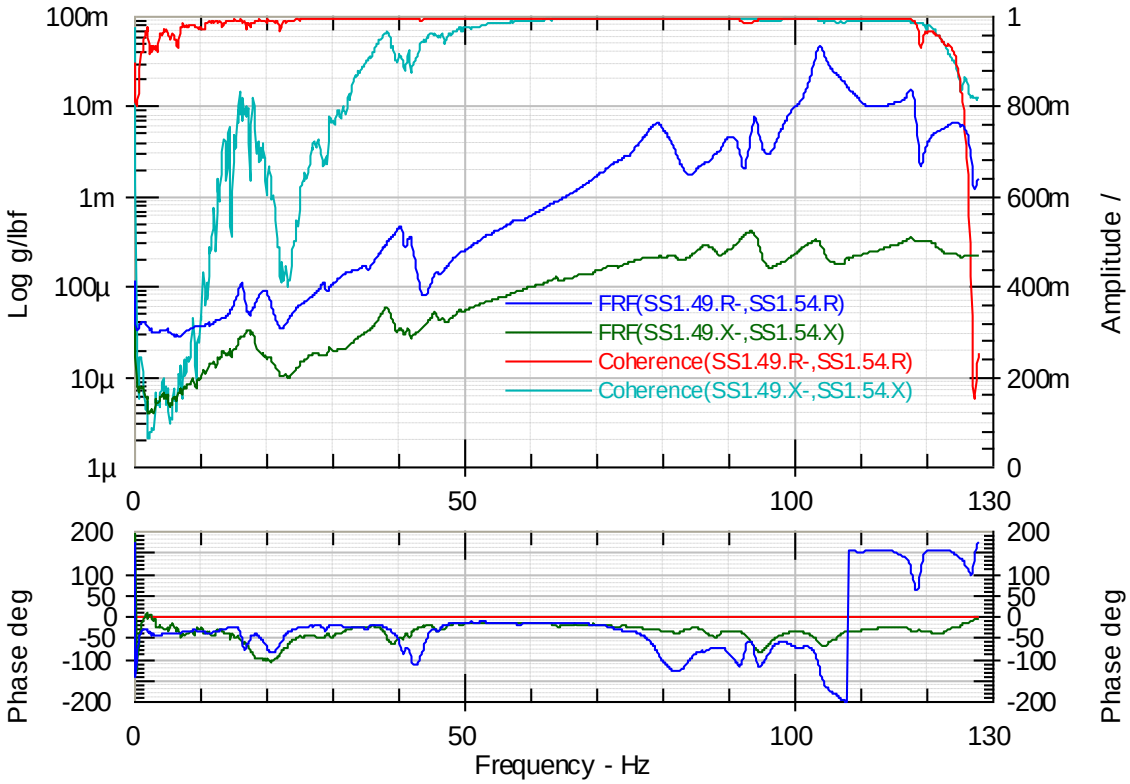

Figure 40. FRF and coherence from impacts at FTS in –R and –X directions

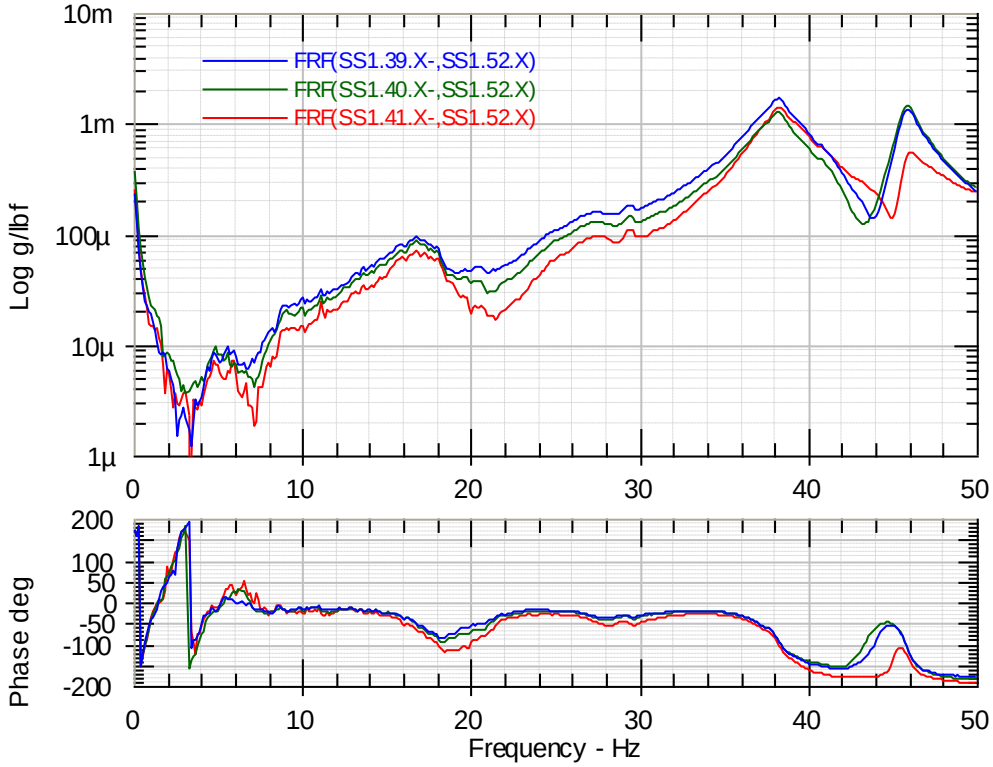

Figure 41. FRF from impacts at IS-1 platform in X direction and response locations 39-41

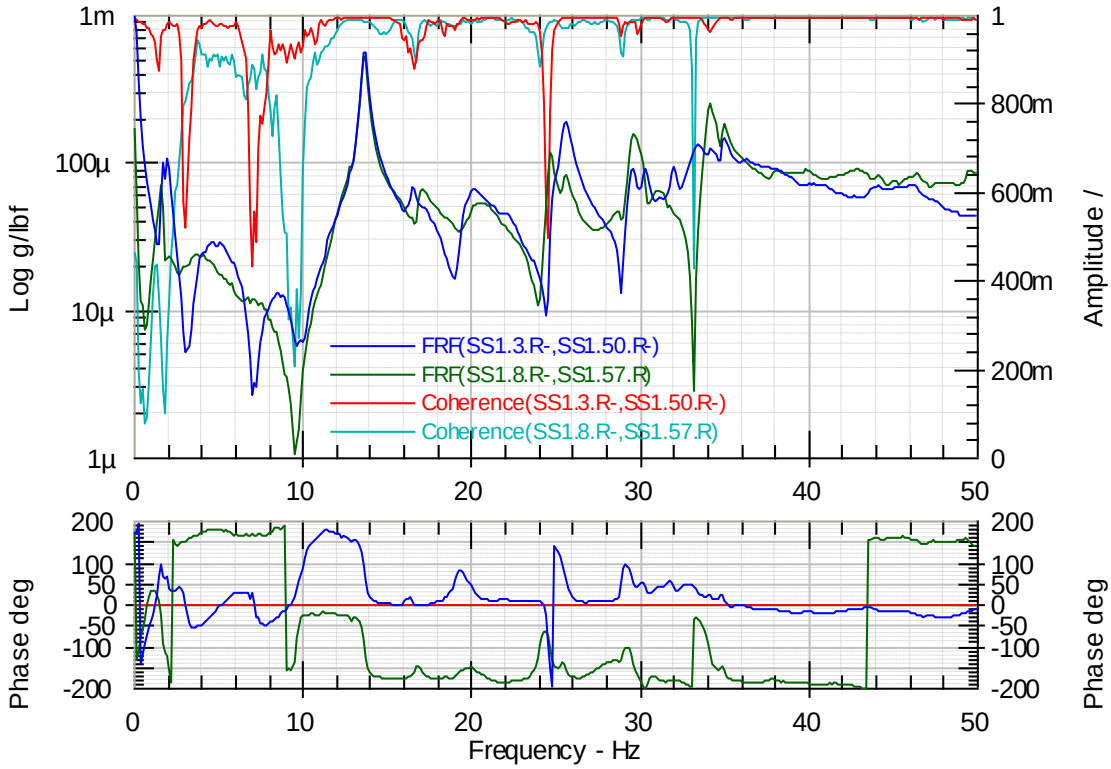

Figure 42. FRF from impacts at frustum

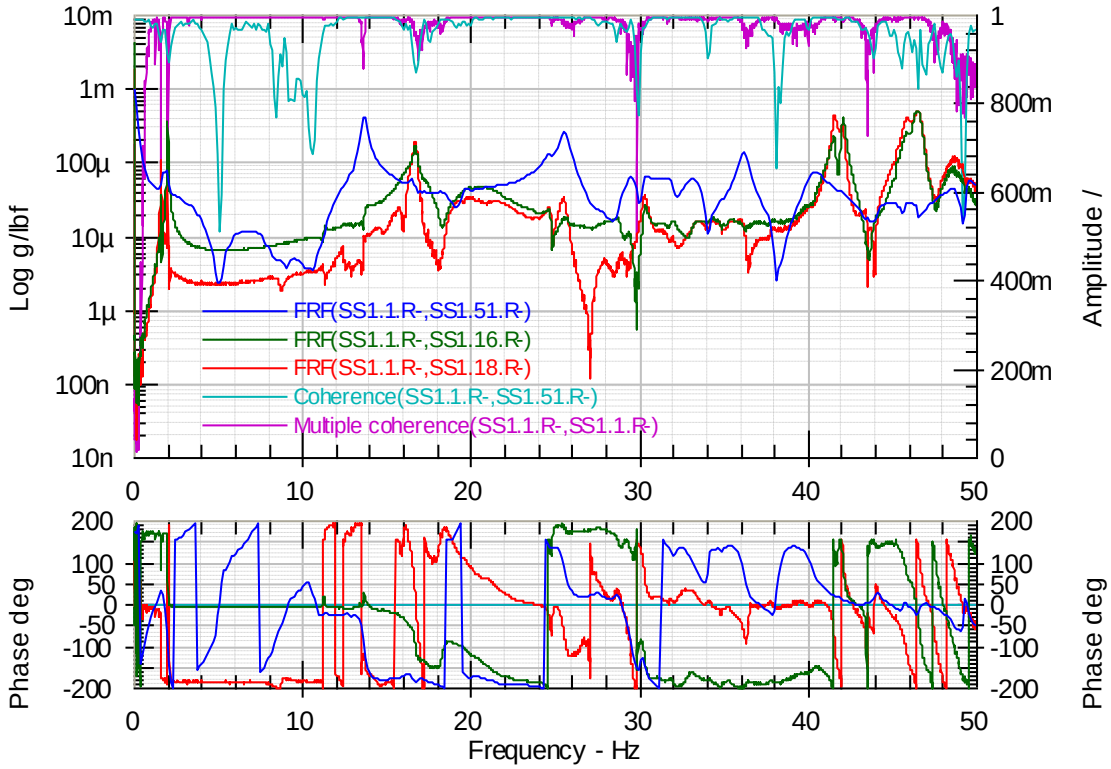

Figure 43. Comparison of FRF and coherence from impact at frustum (51R-) and multi-input random shaker test (16R-, 18R-)

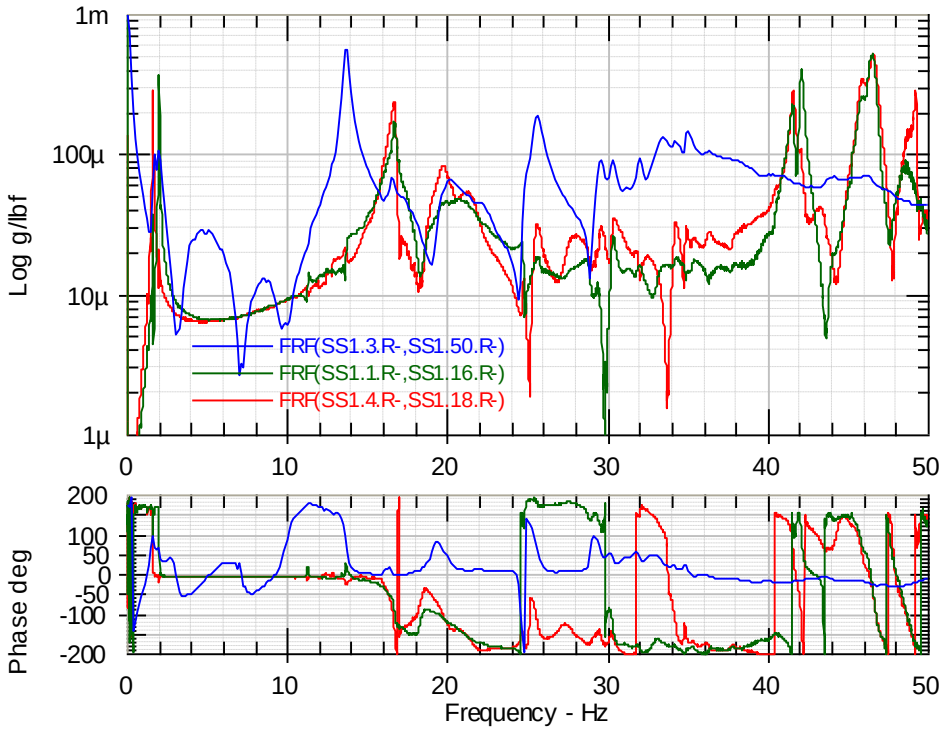

Figure 44. Comparison of FRF from impact at frustum (50R-) and multi-input random shaker test (16R-, 18R-)

5.0 Experimental Modal Analysis Results

Three independent estimates of the modal parameters [9-11] were made using the random data. Individuals performing the modal estimation noted several difficulties associated with nonlinearity and observability of the modes for Stack 1. As was discussed in Section 4, some nonlinearity in the FRF estimates for different excitation levels was observed. It is believed that the unconventional boundary condition was a significant contributor to the nonlinearity. With regard to observability, parameter estimation above 15 Hz was difficult due to many local modes exhibiting shell behavior and possibly modes of uninstrumented hardware. It was known during the pre-test analysis that higher order modes would need to be assessed on a qualitative basis (see Section 2.3). However, late updates to the FEM after instrumentation placement and a much more compliant boundary than assumed in the baseline model further complicated the observability issue. The boundary condition compliance resulted in more axial participation. Since this was not anticipated, the majority of the sensors were optimized for measuring radial or tangential motion, except for instrumentation at the boundary.

Results for the three independent estimates are provide in Table 7 and select mode shapes are shown in Appendix E. The MSFC estimates [9] are primarily from the 20 lb-rms multi-input random test SS1-6(Run 2) with one mode from the higher level multi-input random test SS1-12 added at mode 4. Aerospace Corporation [10] provided a reduced set of modes with frequency estimates from the higher excitation levels and the estimates from LaRC [11] were from a quick on-site assessment of the 50 lb-rms test SS1-7. The Stack 1^{st} bending mode pair and 1^{st} torsion mode were readily identified. For the higher modes, the estimates required more data manipulation and engineering judgment. Only the reduced set of mode estimates that were matched to the target modes (see Table 1 and Figure 4) were included in Table 7. If the measured frequencies of the 1^{st} bending and torsion modes are compared with the pre-test predictions in Table 1, it is obvious that the test boundary condition is significantly more compliant than the pre-test model. Comparisons between test and analysis and a description of the model calibration process can be found in Horta [5].

Table 7 Reduced set of Modal Estimates

Mode	Frequency (Hz) and Damping (% critical) Estimates			Description
	MSFC [9]	Aerospace [10]	LaRC [11]	
1	1.64 Hz, 0.66%	1.65 Hz	1.63 Hz, 0.88%	Stack 1st Bending
2	2.03 Hz, 0.47%	1.99 Hz	2.02 Hz, 0.70%	Stack 1st Bending
3	11.34 Hz, 0.41%	11.31 Hz	11.3 Hz, 0.47%	Torsion
4	13.67, 0.42% (SS1-12)	13.67 Hz		2N Shell mode
5	16.35, 1.98%	16.30 Hz		2nd Bending
6	16.79 Hz, 0.66%	16.76 Hz	16.7 Hz, 0.62% 16.8 Hz, 0.44%	2N Shell mode
7	19.97 Hz, 0.19%	19.48 Hz		2nd Bending
8	24.78 Hz, 0.34%	24.74 Hz	24.8 Hz, 0.39%	3N shell mode
9	25.56 Hz, 0.49%	25.5 Hz	25.6 Hz, 0.83%	3N shell mode

6.0 Summary

A reduced set of test modes was determined from three independent estimates of the modal parameters. Based on a qualitative assessment, all target mode response behavior from Table 1 was captured in the reduced set of test modes. However, the test modes did not exhibit the predicted coupled response for the 2nd bending and 3N shell modes (see modes 7-8 of Table 1). Pre-test analysis frequencies from Table 1 were significantly higher than the measured frequencies for the 1st bending mode pair and 1st torsion mode. These discrepancies are mainly due to the assumed boundary stiffness in the baseline model being significantly higher than the as tested configuration. Comparisons between the Stack 1 pre-test model and measured data as well as a description of the model calibration process can be found in Horta [5, 12]. Horta [5] incorporated the boundary effects using grounded springs in the FEM calibration process. The resulting optimized boundary spring values corrected a problem with the principal directions for the 1st bending mode pair and also reduced the frequency errors. Although high frequency modes were difficult to observe with the limited instrumentation suite, qualitative assessments of test modes with orthogonality values greater than 0.8 revealed that many of these modes resembled modes found in the analysis.

Results from multiple levels of random and sine sweep tests indicated some nonlinearity in the response, which was attributed to the unconventional test boundary condition. This was observed in the FRFs for different random force levels (see Figure 36) and the sine sweep tests. During the sine sweeps, a 3.7% difference in the first mode frequency was measured for a three-time change in force.

Due to limited time between the Stack 1 test and the modal test on the fully integrated Flight Test Vehicle (FTV) on the Mobile Launcher Platform (MLP), efforts were shifted to pre-test preparation for the FTV on MLP configuration. Additional data analysis and model calibration studies could have been performed for the Stack 1 configuration if the FTV test results indicated the need for model updates in this area of the FEM. However, the FTV on MLP test results [2, 5] were consistent with FEM predictions so no further analysis was performed for Stack 1.

Due to concerns over potential local mode resonance with anticipated launch excitation frequencies, accelerometers were added mid-test to evaluate local mode response at the FSAM and FTS locations. Measured frequencies from the FSAM impact tests confirmed predictions of local modes for the FSAM platform. Impact data for the FTS and FTS battery locations were provided to project personnel to evaluate possible local mode tuning issues.

Lessons Learned:

This effort reinforced the need to incorporate well-defined boundary conditions into the modal test. Unknown boundary conditions add test configuration dependent parameters to the FEM calibration process, which are not part of the final set of system parameters needed. For this configuration, the boundary condition was more compliant than anticipated resulting in complications for both the modal parameter estimation (see Section 5.0) and model calibration process [5].

One additional complicating factor for parameter estimation was the residual effects from out of band shell modes (>40 Hz) that dominated the drive point FRFs (see Figure 19). For future tests of cylindrical structures, excitation along a tangential direction should be considered as a means of minimizing this effect.

References:

[1] NASA Fact Sheet, Constellation Program: Ares I-X Flight Test Vehicle, FS-2009-03-007-JSC, 2009. http://www.nasa.gov/pdf/354470main_aresIX_fs_may09.pdf

[2] Buehrle, R. D., Templeton, J. D., Reaves, M. C., Horta, L. G., Bartolotta, P. A., Parks, R. A., Lazor, D. R., and Gaspar, J. L; Ares I-X Flight Test Vehicle: Stack 5 Modal Test, NASA/TM-2010-216183, January 2010

[3] Buehrle, R. D., Templeton, J. D., Reaves, M. C., Horta, L. G., Bartolotta, P. A., Parks, R. A., Lazor, D. R., and Gaspar, J. L; Ares I-X Flight Test Vehicle Modal Test, NASA/TM-2010-216182, January 2010

[4] Tuttle, R., Lollock, J.A, and Hwung, J.S.: "Identifying Goals for Ares I-X Modal Testing," Proceedings of IMAC XXVIII, Jacksonville, FL., February 1-4, 2010.

[5] Horta, L. G., Reaves, M. C., Buehrle, R. D., Templeton, J. D., Lazor, D. R., Gaspar, J. L., Parks, R. A., and Bartolotta, P. A..; Finite Element Model Calibration Approach for Ares I-X, Proceedings of IMAC XXVIII, Jacksonville, Florida, February 1-4, 2010.

[6] Tuttle, R., and Lollock, J. A.; Modal Test Data Adjustment for Interface Compliance, Proceedings of IMAC XXVIII, Jacksonville, Florida, February 1-4, 2010.

[7] Kammer, D. C.; Sensor Placement for On-Orbit Modal Identification and Correlation of Large Space Structures, Journal of Guidance, Volume 14, No. 2, March-April 1991.

[8] Ewins, D.J., Modal Testing: Theory, Practice and Application, 2nd Edition, Research Studies Press Ltd., pp. 231-234, 2000.

[9] Lazor, D. R., and Parks, R. A.; Ares I-X Super Stack 1-Modal Parameter Estimation (MPE) Results, NASA MSFC presentation, August 11, 2009

[10] Lollock, J.A, Tuttle, R., and Hwung, J.S.; Ares I-X SS1 Modal Test Post-test Review, Aerospace Corporation presentation, August 5, 2009

[11] Gaspar, J.L.; Stack 1 Modal Test –Quick Look Data Analysis, NASA LaRC presentation, July 14, 2009

[12] Horta, L. G., Reaves, M. C., Buehrle, R. D., Templeton, J. D., Lazor, D. R., Gaspar, J. L., Parks, R. A., and Bartolotta, P. A..; SS1 Post Test Assessment of Model Correlation, NASA presentation, August 18, 2009

Appendix A: Acronyms and Abbreviations

BNC	**(Bayonet Neill Concelman) coaxial cable connector**
CM	**Crew Module**
CS	**Coordinate System**
CDAS	**Critical Data Acquisition System**
DAS	**Data Acquisition System**
DFT	**Discrete Fourier Transform**
DOF	**Degree of Freedom**
FEM	**Finite Element Model**
FSAM	**First Stage Avionics Module**
FTINU	**Fault Tolerant Inertial Navigation Unit**
FRF	**Frequency Response Function**
FTS	**Flight Termination System**
FTV	**Flight Test Vehicle**
GRC	**Glenn Research Center**
GSE	**Ground Support Equipment**
HPS	**Hydraulic Power Supply**
Hz	**Hertz**
IEEE	**Institute of Electrical and Electronics Engineers**
IEPE	**Integrated Electronics Piezo Electric**
IPT's	**Integrated Product Teams**
IS	**Interstage**
IVM	**Integrated Vehicle Model**
HB	**High Bay**
KSC	**Kennedy Space Center**
LaRC	**Langley Research Center**
LAS	**Launch Abort System**
lb	**Pound**

LVDT	**Linear Variable Displacement Transducer**
MIMO	**Multi-Input Multi-Output**
MLP	**Mobile Launcher Platform**
MSFC	**Marshall Space Flight Center**
pk	**Peak**
psi	**Pounds per square inch**
PV	**Principal Value**
rms	**Root Mean Square**
RRGU	**Redundant Rate Gyro Unit**
SA	**Spacecraft Adapter**
SE&I	**Systems Engineering & Integration**
SM	**Service Module**
SSAS	**Super-Segment Assembly Stand**
STDev	**Standard Deviation**
STI	**Scientific and Technical Information**
TBD	**To Be Determined**
TBR	**To Be Resolved**
UPS	**Uninterrupted Power Supply**
USS	**Upper Stage Simulator**
VAB	**Vehicle Assembly Building**
VXI	**VME eXtensions for Instrumentation**

Appendix B: Equipment List

Table B.1. FTV Equipment List (1 of 3)

	DATA ACQUISITION SYSTEM (DAS) RACK							
NAME	**MANUFACTURER**	**MODEL**	**SERIAL**	**OWNER**	**QTY**	**CAL DATE**	**CAL DUE**	**MISC**
VXI MAINFRAME	AGILENT TECHNOLOGIES	E8403A	US38001676	LaRC	1	n/a	n/a	
SLOT-0 INTERFACE	AGILENT TECHNOLOGIES	E8491A	US39007039	LaRC	1	n/a	n/a	VXI 0
16 CHANNEL DIGITIZER	VXI TECHNOLOGY INC	VT1432B	US45004211	LaRC	1	6/26/2009	6/26/2011	VXI 1
16 CHANNEL DIGITIZER	VXI TECHNOLOGY INC	VT1432B	US45004212	LaRC	1	6/26/2009	6/26/2011	VXI 2
16 CHANNEL DIGITIZER	VXI TECHNOLOGY INC	VT1432B	US45004209	LaRC	1	6/26/2009	6/26/2011	VXI 3
16 CHANNEL DIGITIZER	VXI TECHNOLOGY INC	VT1432B	US45004210	LaRC	1	6/26/2009	6/26/2011	VXI 4
16 CHANNEL DIGITIZER	VXI TECHNOLOGY INC	VT1432B	US45004537	LaRC	1	1/22/2008	1/22/2010	VXI 5
16 CHANNEL DIGITIZER	VXI TECHNOLOGY INC	VT1432B	US45004538	LaRC	1	1/22/2008	1/22/2010	VXI 6
4 CHANNEL SOURCE MODULE	HEWLETT-PACKARD CO	E1434A	US37260104	LaRC	1	n/a	n/a	VXI 7
16 CHANNEL DIGITIZER WITH SOURCE	VXI TECHNOLOGY INC	VT1432B	US45004540	LaRC	1	1/22/2008	1/22/2010	VXI 8
DIGITAL OSCILLOSCOPE	TEKTRONIX	TDS2014	C014678	LaRC	1	n/a	n/a	
ICP/VOLTAGE 8CH INPUT BOX	AGILENT TECHNOLOGIES	3241A	n/a	LaRC	4	n/a	n/a	
VOLTAGE 8CH INPUT BOX	HEWLETT-PACKARD CO	3240A	n/a	LaRC	4	n/a	n/a	
	SIGNAL CONDITIONER (S/C) RACK							
NAME	**MANUFACTURER**	**MODEL**	**SERIAL**	**OWNER**	**QTY**	**CAL DATE**	**CAL DUE**	**MISC**
ICP SIGNAL CONDITIONER	PCB PIEZOTRONICS	584A	1135	LaRC	1	2/9/2009	2/9/2010	S/C 1
CAPACITIVE SIGNAL CONDITIONER	PCB PIEZOTRONICS	478A16	151	LaRC	1	11/7/2008	11/7/2009	S/C 2
CAPACITIVE SIGNAL CONDITIONER	PCB PIEZOTRONICS	478A16	157	MSFC	1	1/12/2009	1/12/2010	S/C 3
CAPACITIVE SIGNAL CONDITIONER	PCB PIEZOTRONICS	478A16	154	MSFC	1	3/10/2009	3/10/2010	S/C 4
CAPACITIVE SIGNAL CONDITIONER	PCB PIEZOTRONICS	478A16	312	MSFC	1	1/12/2009	1/12/2010	S/C 5
CAPACITIVE SIGNAL CONDITIONER	PCB PIEZOTRONICS	478A16	311	MSFC	1	1/12/2009	1/12/2010	S/C 6
CAPACITIVE SIGNAL CONDITIONER	PCB PIEZOTRONICS	478A16	290	MSFC	1	6/24/2009	12/24/2009	S/C 7
BANDPASS FILTER	KROHN-HITE	3343	2080	LaRC	1	4/20/2009	4/20/2011	Shaker 1
BANDPASS FILTER	KROHN-HITE	3343R	479	LaRC	1	3/11/2009	3/11/2011	Shaker 2
	ICP INSTRUMENTATION							
NAME	**MANUFACTURER**	**MODEL**	**SERIAL**	**OWNER**	**QTY**	**CAL DATE**	**CAL DUE**	**SENS**
IMPACT HAMMER	PCB PIEZOTRONICS	086B20	4095	LaRC	1	4/9/2009	4/9/2010	1.08 mV/lbf
IMPEDANCE HEAD	PCB PIEZOTRONICS	288M34	1785	MSFC	1	2/10/2009	2/10/2010	9.837 mV/lbf
V	V	V	1785	MSFC	1	2/10/2009	2/10/2010	99.0 mV/g
IMPEDANCE HEAD	PCB PIEZOTRONICS	288M34	1783	MSFC	1	2/10/2009	2/10/2010	9.915 mV/lbf
V	V	V	1783	MSFC	1	2/10/2009	2/10/2010	100.3 mV/g

Table B.1. FTV Equipment List (2 of 3)

MSFC ACCELEROMETERS									
NAME	MANUFACTURER	MODEL	SERIAL	OWNER	QTY	CAL DATE	CAL DUE	159.2Hz SENS (mV/g)	DC SENS (mV/g)
CAPACITIVE ACCELEROMETER	PCB PIEZOTRONICS	3701M15	2562	MSFC	1	1/21/2009	1/21/2010	998	975
CAPACITIVE ACCELEROMETER	PCB PIEZOTRONICS	3701M15	2563	MSFC	1	1/21/2009	1/21/2010	1050	988
CAPACITIVE ACCELEROMETER	PCB PIEZOTRONICS	3701M15	2567	MSFC	1	1/22/2009	1/22/2010	1020	989
CAPACITIVE ACCELEROMETER	PCB PIEZOTRONICS	3701M15	2569	MSFC	1	1/21/2009	1/21/2010	1000	991
CAPACITIVE ACCELEROMETER	PCB PIEZOTRONICS	3701M15	2570	MSFC	1	1/21/2009	1/21/2010	964	980
CAPACITIVE ACCELEROMETER	PCB PIEZOTRONICS	3701M15	2571	MSFC	1	1/21/2009	1/21/2010	975	982
CAPACITIVE ACCELEROMETER	PCB PIEZOTRONICS	3701M15	2576	MSFC	1	1/21/2009	1/21/2010	991	975
CAPACITIVE ACCELEROMETER	PCB PIEZOTRONICS	3701M15	2577	MSFC	1	1/21/2009	1/21/2010	1050	989
CAPACITIVE ACCELEROMETER	PCB PIEZOTRONICS	3701M15	2578	MSFC	1	1/22/2009	1/22/2010	983	984
CAPACITIVE ACCELEROMETER	PCB PIEZOTRONICS	3701M15	2579	MSFC	1	1/21/2009	1/21/2010	1020	984
CAPACITIVE ACCELEROMETER	PCB PIEZOTRONICS	3701M15	2580	MSFC	1	1/21/2009	1/21/2010	1040	990
CAPACITIVE ACCELEROMETER	PCB PIEZOTRONICS	3701M15	2581	MSFC	1	1/21/2009	1/21/2010	1040	988
CAPACITIVE ACCELEROMETER	PCB PIEZOTRONICS	3701M15	2582	MSFC	1	1/21/2009	1/21/2010	1040	997
CAPACITIVE ACCELEROMETER	PCB PIEZOTRONICS	3701M15	2583	MSFC	1	1/21/2009	1/21/2010	1040	986
CAPACITIVE ACCELEROMETER	PCB PIEZOTRONICS	3701M15	2584	MSFC	1	1/22/2009	1/22/2010	1030	983
CAPACITIVE ACCELEROMETER	PCB PIEZOTRONICS	3701M15	2585	MSFC	1	1/22/2009	1/22/2010	996	992
CAPACITIVE ACCELEROMETER	PCB PIEZOTRONICS	3701M15	2586	MSFC	1	1/22/2009	1/22/2010	999	981
CAPACITIVE ACCELEROMETER	PCB PIEZOTRONICS	3701M15	2587	MSFC	1	1/21/2009	1/21/2010	1030	991
CAPACITIVE ACCELEROMETER	PCB PIEZOTRONICS	3701M15	2588	MSFC	1	1/22/2009	1/22/2010	1020	978
CAPACITIVE ACCELEROMETER	PCB PIEZOTRONICS	3701M15	2589	MSFC	1	1/21/2009	1/21/2010	979	983
CAPACITIVE ACCELEROMETER	PCB PIEZOTRONICS	3701M15	2591	MSFC	1	1/22/2009	1/22/2010	1040	990
CAPACITIVE ACCELEROMETER	PCB PIEZOTRONICS	3701M15	2592	MSFC	1	1/21/2009	1/21/2010	1040	986
CAPACITIVE ACCELEROMETER	PCB PIEZOTRONICS	3701M15	2595	MSFC	1	1/22/2009	1/22/2010	1010	995
CAPACITIVE ACCELEROMETER	PCB PIEZOTRONICS	3701M15	2596	MSFC	1	1/22/2009	1/22/2010	1040	988
CAPACITIVE ACCELEROMETER	PCB PIEZOTRONICS	3701M15	2597	MSFC	1	1/21/2009	1/21/2010	1040	997
CAPACITIVE ACCELEROMETER	PCB PIEZOTRONICS	3701M15	2598	MSFC	1	1/21/2009	1/21/2010	1020	1000
CAPACITIVE ACCELEROMETER	PCB PIEZOTRONICS	3701M15	2599	MSFC	1	1/21/2009	1/21/2010	974	991
CAPACITIVE ACCELEROMETER	PCB PIEZOTRONICS	3701M15	2601	MSFC	1	1/22/2009	1/22/2010	1000	988
CAPACITIVE ACCELEROMETER	PCB PIEZOTRONICS	3701M15	2603	MSFC	1	1/21/2009	1/21/2010	1030	984
CAPACITIVE ACCELEROMETER	PCB PIEZOTRONICS	3701M15	2605	MSFC	1	1/22/2009	1/22/2010	987	984
CAPACITIVE ACCELEROMETER	PCB PIEZOTRONICS	3701M15	2606	MSFC	1	1/22/2009	1/22/2010	1020	987
CAPACITIVE ACCELEROMETER	PCB PIEZOTRONICS	3701M15	2607	MSFC	1	1/22/2009	1/22/2010	1010	983
CAPACITIVE ACCELEROMETER	PCB PIEZOTRONICS	3701M15	2608	MSFC	1	1/22/2009	1/22/2010	1010	985
CAPACITIVE ACCELEROMETER	PCB PIEZOTRONICS	3701M15	2609	MSFC	1	1/21/2009	1/21/2010	1030	981
CAPACITIVE ACCELEROMETER	PCB PIEZOTRONICS	3701M15	2610	MSFC	1	1/22/2009	1/22/2010	1000	983
CAPACITIVE ACCELEROMETER	PCB PIEZOTRONICS	3701M15	2611	MSFC	1	1/21/2009	1/21/2010	1020	994
CAPACITIVE ACCELEROMETER	PCB PIEZOTRONICS	3701M15	2612	MSFC	1	1/21/2009	1/21/2010	1040	988
CAPACITIVE ACCELEROMETER	PCB PIEZOTRONICS	3701M15	2613	MSFC	1	1/21/2009	1/21/2010	1010	995
CAPACITIVE ACCELEROMETER	PCB PIEZOTRONICS	3701M15	2614	MSFC	1	1/22/2009	1/22/2010	1040	974
CAPACITIVE ACCELEROMETER	PCB PIEZOTRONICS	3701M15	2615	MSFC	1	1/22/2009	1/22/2010	1050	992
CAPACITIVE ACCELEROMETER	PCB PIEZOTRONICS	3701M15	2670	MSFC	1	1/22/2009	1/22/2010	1050	992
CAPACITIVE ACCELEROMETER	PCB PIEZOTRONICS	3701M15	2671	MSFC	1	1/22/2009	1/22/2010	1030	984
CAPACITIVE ACCELEROMETER	PCB PIEZOTRONICS	3701M15	2672	MSFC	1	1/21/2009	1/21/2010	991	986
CAPACITIVE ACCELEROMETER	PCB PIEZOTRONICS	3701M15	2673	MSFC	1	1/22/2009	1/22/2010	1030	985
CAPACITIVE ACCELEROMETER	PCB PIEZOTRONICS	3701M15	2675	MSFC	1	1/22/2009	1/22/2010	1030	988
CAPACITIVE ACCELEROMETER	PCB PIEZOTRONICS	3701M15	2676	MSFC	1	1/21/2009	1/21/2010	943	991
CAPACITIVE ACCELEROMETER	PCB PIEZOTRONICS	3701M15	2679	MSFC	1	1/22/2009	1/22/2010	1030	981
CAPACITIVE ACCELEROMETER	PCB PIEZOTRONICS	3701M15	8138	MSFC	1	1/21/2009	1/21/2010	1010	976
CAPACITIVE ACCELEROMETER	PCB PIEZOTRONICS	3701M15	8139	MSFC	1	1/21/2009	1/21/2010	985	977
CAPACITIVE ACCELEROMETER	PCB PIEZOTRONICS	3701M15	8140	MSFC	1	1/21/2009	1/21/2010	1060	1020
CAPACITIVE ACCELEROMETER	PCB PIEZOTRONICS	3701M15	8141	MSFC	1	1/21/2009	1/21/2010	1010	977
CAPACITIVE ACCELEROMETER	PCB PIEZOTRONICS	3701M15	8142	MSFC	1	1/21/2009	1/21/2010	1020	999
CAPACITIVE ACCELEROMETER	PCB PIEZOTRONICS	3701M15	8156	MSFC	1	1/21/2009	1/21/2010	941	990
CAPACITIVE ACCELEROMETER	PCB PIEZOTRONICS	3701M15	8157	MSFC	1	1/21/2009	1/21/2010	977	999

Table B.1. FTV Equipment List (3 of 3)

CAPACITIVE ACCELEROMETER	PCB PIEZOTRONICS	3701M15	8158	MSFC	1	1/21/2009	1/21/2010	1010	987
CAPACITIVE ACCELEROMETER	PCB PIEZOTRONICS	3701M15	8159	MSFC	1	1/21/2009	1/21/2010	1010	997
CAPACITIVE ACCELEROMETER	PCB PIEZOTRONICS	3701M15	8160	MSFC	1	1/21/2009	1/21/2010	994	983
CAPACITIVE ACCELEROMETER	PCB PIEZOTRONICS	3701M15	8161	MSFC	1	1/21/2009	1/21/2010	932	980
CAPACITIVE ACCELEROMETER	PCB PIEZOTRONICS	3701M15	8162	MSFC	1	1/21/2009	1/21/2010	941	965
CAPACITIVE ACCELEROMETER	PCB PIEZOTRONICS	3701M15	8163	MSFC	1	1/21/2009	1/21/2010	1030	981
CAPACITIVE ACCELEROMETER	PCB PIEZOTRONICS	3701M15	8164	MSFC	1	1/21/2009	1/21/2010	972	1000
CAPACITIVE ACCELEROMETER	PCB PIEZOTRONICS	3701M15	8165	MSFC	1	1/21/2009	1/21/2010	986	980
CAPACITIVE ACCELEROMETER	PCB PIEZOTRONICS	3701M15	8166	MSFC	1	1/21/2009	1/21/2010	979	992
CAPACITIVE ACCELEROMETER	PCB PIEZOTRONICS	3701M15	8167	MSFC	1	1/21/2009	1/21/2010	1040	989
CAPACITIVE ACCELEROMETER	PCB PIEZOTRONICS	3701M15	8168	MSFC	1	1/21/2009	1/21/2010	998	984
CAPACITIVE ACCELEROMETER	PCB PIEZOTRONICS	3701M15	8169	MSFC	1	1/21/2009	1/21/2010	1040	990
CAPACITIVE ACCELEROMETER	PCB PIEZOTRONICS	3701M15	8170	MSFC	1	1/21/2009	1/21/2010	1010	981
CAPACITIVE ACCELEROMETER	PCB PIEZOTRONICS	3701M15	8171	MSFC	1	1/21/2009	1/21/2010	975	985
CAPACITIVE ACCELEROMETER	PCB PIEZOTRONICS	3701M15	8172	MSFC	1	1/22/2009	1/22/2010	981	984
CAPACITIVE ACCELEROMETER	PCB PIEZOTRONICS	3701M15	8173	MSFC	1	1/21/2009	1/21/2010	961	979
CAPACITIVE ACCELEROMETER	PCB PIEZOTRONICS	3701M15	8174	MSFC	1	1/21/2009	1/21/2010	951	972
CAPACITIVE ACCELEROMETER	PCB PIEZOTRONICS	3701M15	8175	MSFC	1	1/21/2009	1/21/2010	962	999
CAPACITIVE ACCELEROMETER	PCB PIEZOTRONICS	3701M15	8176	MSFC	1	1/21/2009	1/21/2010	929	984
CAPACITIVE ACCELEROMETER	PCB PIEZOTRONICS	3701M15	8177	MSFC	1	1/21/2009	1/21/2010	961	983
CAPACITIVE ACCELEROMETER	PCB PIEZOTRONICS	3701M15	8178	MSFC	1	1/21/2009	1/21/2010	1090	981
CAPACITIVE ACCELEROMETER	PCB PIEZOTRONICS	3701M15	8179	MSFC	1	1/21/2009	1/21/2010	978	980
CAPACITIVE ACCELEROMETER	PCB PIEZOTRONICS	3701M15	8180	MSFC	1	1/21/2009	1/21/2010	992	994
CAPACITIVE ACCELEROMETER	PCB PIEZOTRONICS	3701M15	8181	MSFC	1	1/21/2009	1/21/2010	1040	988
CAPACITIVE ACCELEROMETER	PCB PIEZOTRONICS	3701M15	8182	MSFC	1	1/21/2009	1/21/2010	1000	996
CAPACITIVE ACCELEROMETER	PCB PIEZOTRONICS	3711D1FA3G	517	MSFC	1	1/22/2009	1/22/2010	658	702
CAPACITIVE ACCELEROMETER	PCB PIEZOTRONICS	3711D1FA3G	518	MSFC	1	1/22/2009	1/22/2010	661	694
CAPACITIVE ACCELEROMETER	PCB PIEZOTRONICS	3711D1FA3G	519	MSFC	1	1/22/2009	1/22/2010	659	696
	LAS PRE-INSTALLED ACCELEROMETERS								
NAME	**MANUFACTURER**	**MODEL**	**SERIAL**	**OWNER**	**QTY**	**CAL DATE**	**CAL DUE**	**30Hz SENS (mV/g)**	**DC SENS (mV/g)**
CAPACITIVE ACCELEROMETER	PCB PIEZOTRONICS	3701G3FA3G	2020	LaRC	1	10/1/2008	10/1/2009	991.25	996.6
CAPACITIVE ACCELEROMETER	PCB PIEZOTRONICS	3701G3FA3G	2021	LaRC	1	9/29/2008	9/29/2009	998.74	1009.3
CAPACITIVE ACCELEROMETER	PCB PIEZOTRONICS	3701G3FA3G	2022	LaRC	1	10/1/2008	10/1/2009	998.93	995.9
CAPACITIVE ACCELEROMETER	PCB PIEZOTRONICS	3701G3FA3G	2023	LaRC	1	10/1/2008	10/1/2009	996.69	991.0
CAPACITIVE ACCELEROMETER	PCB PIEZOTRONICS	3701G3FA3G	2026	LaRC	1	9/29/2008	9/29/2009	993.12	991.0
CAPACITIVE ACCELEROMETER	PCB PIEZOTRONICS	3701G3FA3G	2027	LaRC	1	9/29/2008	9/29/2009	997.99	1003.9

Appendix C: Instrumentation Setup and Channel Mapping

Table C.1. Instrumentation Locations

	As-Installed Geometry			
Location	Radial (in)	Theta (deg)	Z-coord (in)	Notes
1	108.25	30	1859.5	
2	108.25	60	1858.7	
3	108.25	105	1860	
4	108.25	150	1859.2	
5	108.25	195	1860.5	
6	108.25	240	1858.2	
7	108.25	300	1860	
8	108.25	345	1860.5	R & T were switched in SS1-6 time data
9	108.25	30	1939.2	
10	108.25	135	1938.5	
11	108.25	192	1937.5	
12	108.25	225	1939.3	
13	108.25	348	1937.2	
14	72.79	195	2137	
15	72.79	225	2137	
16	72.79	40	2335.9	Shaker 1 location
17	72.79	112.5	2328.3	
18	72.79	140	2336.4	Shaker 2 location
19	72.79	210	2327.7	
20	72.79	232.5	2328.1	
21	72.79	300	2327.7	
22	72.79	330	2327.2	
23	72.79	45	2601.6	
24	72.79	135	2601.6	
25	72.79	225	2601.6	
26	72.79	315	2601.6	
27	72.79	45	2592.5	
28	72.79	135	2592.5	
29	72.79	225	2592.6	
30	72.79	315	2592.4	
31	72.79	47	2602.9	
32	72.79	133	2602.9	
33	72.79	228	2602.9	
34	72.79	313	2602.9	
35	72.79	0	2602.9	
36	72.79	90	2602.9	
37	72.79	180	2602.9	
38	72.79	270	2602.9	
39	0	0	1971	Center of IS-1 Platform
40	54	315	1971	IS-1 Platform: 54.0" from Center
41	54.6	45	1971	IS-1 Platform: 54.6" from Center
42	72.79	40	2335.9	Impedance head accelerometer at location 16
43	72.79	140	2336.4	Impedance head accelerometer at location 18
44				Unused
45				Unused
46	45	150	2480.9	FSAM-27 Inches from Center Ring. Not connected until SS1-12 test.
47	21.25	150	2480.9	FSAM-3.25 Inches from Center Ring. Not connected until SS1-12 test
48	66.79	210	2534.9	battery -radius estimated. Not connected until SS1-12 test
49	69.79	65	2569.9	FTS -radius estimated. Not connected until SS1-12 test

Table C.2. Instrumentation Orientations

	X-Axis Accel		Radial (R) Accel		Tangential (T) Accel		Load Cell	
Location	Orientation	S/N	Orientation	S/N	Orientation	S/N	Orientation	S/N
1			-R	2589	T	2580		
2			-R	2592	T	8174		
3			-R	2676	T	2671		
4			-R	2605	T	2606		
5			-R	8159	T	8168		
6			-R	2675	T	2596		
7			-R	8140	T	8164		
8			-R	2563	T	2615		
9			-R	8139	T	8181		
10			-R	2611	T	2571		
11			-R	2607	T	2585		
12			-R	2588	T	2595		
13			-R	8177	T	2603		
14			R	8169	T	8179		
15			R	2583	T	2609		
16			R	2614	T	2673	R-	1785
17			R	2578	T	2586		
18			R	8161	T	8176	R-	1783
19			R	2610	T	2608		
20			R	8157	T	2582		
21			R	8156	T	8171		
22			R	2601	T	2584		
23	-X	8158	R	8141	T	8162		
24	-X	2597	R	8180				
25	-X	8167	R	2579	T	8138		
26	-X	2591	R	2679				
27	-X	8182						
28	-X	8170						
29	-X	2569						
30	-X	2598						
31	-X	2570	R	2576	T	8163		
32	-X	8172	R	8173				
33	-X	2562	R	8142	T	8160		
34	-X	2587	R	8165				
35	-X	8166						
36	-X	2577						
37	-X	8178						
38	-X	2599						
39	-X	2670	R	2613	T	2672		
40	-X	2581			T	2612		
41	-X	8175						
42			R	1785				
43			R	1783				
44								
45								
46	X	3021	-R	2028	T	2029		
47	X	3051	-R	3025	T	3022		
48	-X	518	-R	519				
49	-X	2096	-R	2095				

Table C.3. Transducer Channel Setup (1 of 2)

TRANSDUCER CHANNELS								
Channel	**Usage**	**Name**	**EU**	**Sensitivity**	**Cal Type**	**Input Mod**	**Model**	**Serial**
1	Excitation	SS1.16.R-	lbf	9.837	mV/EU	Voltage	288M34	1785
2	Excitation	SS1.18.R-	lbf	9.915	mV/EU	Voltage	288M34	1783
3	Response	SS1.16.R	g	974	mV/EU	Voltage	3701M15	2614
4	Response	SS1.18.R	g	980	mV/EU	Voltage	3701M15	8161
5	Response	SS1.1.R-	g	983	mV/EU	Voltage	3701M15	2589
6	Response	SS1.1.T	g	990	mV/EU	Voltage	3701M15	2580
7	Response	SS1.2.R-	g	986	mV/EU	Voltage	3701M15	2592
8	Response	SS1.2.T	g	972	mV/EU	Voltage	3701M15	8174
9	Response	SS1.3.R-	g	991	mV/EU	Voltage	3701M15	2676
10	Response	SS1.3.T	g	984	mV/EU	Voltage	3701M15	2671
11	Response	SS1.4.R-	g	984	mV/EU	Voltage	3701M15	2605
12	Response	SS1.4.T	g	987	mV/EU	Voltage	3701M15	2606
13	Response	SS1.5.R-	g	997	mV/EU	Voltage	3701M15	8159
14	Response	SS1.5.T	g	984	mV/EU	Voltage	3701M15	8168
15	Response	SS1.6.R-	g	988	mV/EU	Voltage	3701M15	2675
16	Response	SS1.6.T	g	988	mV/EU	Voltage	3701M15	2596
17	Response	SS1.7.R-	g	1020	mV/EU	Voltage	3701M15	8140
18	Response	SS1.7.T	g	1000	mV/EU	Voltage	3701M15	8164
19	Response	SS1.8.T	g	988	mV/EU	Voltage	3701M15	2563
20	Response	SS1.8.R-	g	992	mV/EU	Voltage	3701M15	2615
21	Response	SS1.9.R-	g	977	mV/EU	Voltage	3701M15	8139
22	Response	SS1.9.T	g	988	mV/EU	Voltage	3701M15	8181
23	Response	SS1.10.R-	g	994	mV/EU	Voltage	3701M15	2611
24	Response	SS1.10.T	g	982	mV/EU	Voltage	3701M15	2571
25	Response	SS1.11.R-	g	983	mV/EU	Voltage	3701M15	2607
26	Response	SS1.11.T	g	992	mV/EU	Voltage	3701M15	2585
27	Response	SS1.12.R-	g	978	mV/EU	Voltage	3701M15	2588
28	Response	SS1.12.T	g	995	mV/EU	Voltage	3701M15	2595
29	Response	SS1.13.R-	g	983	mV/EU	Voltage	3701M15	8177
30	Response	SS1.13.T	g	984	mV/EU	Voltage	3701M15	2603
31	Response	SS1.14.R	g	990	mV/EU	Voltage	3701M15	8169
32	Response	SS1.14.T	g	980	mV/EU	Voltage	3701M15	8179
33	Response	SS1.15.R	g	986	mV/EU	Voltage	3701M15	2583
34	Response	SS1.15.T	g	981	mV/EU	Voltage	3701M15	2609
35	Response	SS1.16.T	g	985	mV/EU	Voltage	3701M15	2673
36	Response	SS1.17.R	g	984	mV/EU	Voltage	3701M15	2578
37	Response	Open	g	1000	mV/EU	Voltage	NA	NA
38	Response	SS1.18.T	g	984	mV/EU	Voltage	3701M15	8176
39	Response	SS1.19.R	g	983	mV/EU	Voltage	3701M15	2610
40	Response	SS1.19.T	g	985	mV/EU	Voltage	3701M15	2608
41	Response	Open	g	1000	mV/EU	Voltage	NA	NA
42	Response	Open	g	1000	mV/EU	Voltage	NA	NA
43	Response	Open	g	1000	mV/EU	Voltage	NA	NA
44	Response	Open	g	1000	mV/EU	Voltage	NA	NA
45	Response	SS1.22.R	g	988	mV/EU	Voltage	3701M15	2601
46	Response	SS1.22.T	g	983	mV/EU	Voltage	3701M15	2584
47	Response	SS1.23.X-	g	987	mV/EU	Voltage	3701M15	8158
48	Response	SS1.23.R	g	977	mV/EU	Voltage	3701M15	8141
49	Response	SS1.23.T	g	965	mV/EU	Voltage	3701M15	8162
50	Response	SS1.24.X-	g	997	mV/EU	Voltage	3701M15	2597
51	Response	SS1.24.R	g	994	mV/EU	Voltage	3701M15	8180

Table C.3. Transducer Channel Setup (2 of 2)

TRANSDUCER CHANNELS								
Channel	Usage	Name	EU	Sensitivity	Cal Type	Input Mod	Model	Serial
52	Response	SS1.25.X-	g	989	mV/EU	Voltage	3701M15	8167
53	Response	SS1.25.R	g	984	mV/EU	Voltage	3701M15	2579
54	Response	SS1.25.T	g	976	mV/EU	Voltage	3701M15	8138
55	Response	SS1.26.X-	g	990	mV/EU	Voltage	3701M15	2591
56	Response	SS1.26.R	g	981	mV/EU	Voltage	3701M15	2679
57	Response	SS1.27.X-	g	996	mV/EU	Voltage	3701M15	8182
58	Response	SS1.28.X-	g	981	mV/EU	Voltage	3701M15	8170
59	Response	SS1.29.X-	g	991	mV/EU	Voltage	3701M15	2569
60	Response	SS1.30.X-	g	1000	mV/EU	Voltage	3701M15	2598
61	Response	SS1.31.X-	g	980	mV/EU	Voltage	3701M15	2570
62	Response	SS1.31.R	g	975	mV/EU	Voltage	3701M15	2576
63	Response	SS1.31.T	g	981	mV/EU	Voltage	3701M15	8163
64	Response	SS1.32.X-	g	984	mV/EU	Voltage	3701M15	8172
65	Response	SS1.32.R	g	979	mV/EU	Voltage	3701M15	8173
66	Response	SS1.33.X-	g	975	mV/EU	Voltage	3701M15	2562
67	Response	SS1.33.R	g	999	mV/EU	Voltage	3701M15	8142
68	Response	SS1.33.T	g	983	mV/EU	Voltage	3701M15	8160
69	Response	SS1.34.X-	g	991	mV/EU	Voltage	3701M15	2587
70	Response	SS1.34.R	g	980	mV/EU	Voltage	3701M15	8165
71	Response	SS1.35.X-	g	992	mV/EU	Voltage	3701M15	8166
72	Response	SS1.36.X-	g	989	mV/EU	Voltage	3701M15	2577
73	Response	SS1.37.X-	g	981	mV/EU	Voltage	3701M15	8178
74	Response	SS1.38.X-	g	991	mV/EU	Voltage	3701M15	2599
75	Response	SS1.42.R	g	99	mV/EU	Voltage	288M34	1785
76	Response	SS1.43.R	g	100.3	mV/EU	Voltage	288M34	1783
77	Response	SS1.17.T	g	981	mV/EU	Voltage	3701M15	2586
78	Response	Open	g	1000	mV/EU	Voltage	NA	NA
79	Response	Open	g	1000	mV/EU	Voltage	NA	NA
80	Response	Open	g	1000	mV/EU	Voltage	NA	NA
81	Response	Open	g	1000	mV/EU	Voltage	NA	NA
82	Response	Open	g	1000	mV/EU	Voltage	NA	NA
83	Response	SS1.39.X-	g	992	mV/EU	Voltage	3701M15	2670
84	Response	SS1.39.R	g	995	mV/EU	Voltage	3701M15	2613
85	Response	SS1.39.T	g	986	mV/EU	Voltage	3701M15	2672
86	Response	SS1.40.X-	g	988	mV/EU	Voltage	3701M15	2581
87	Response	SS1.40.T	g	988	mV/EU	Voltage	3701M15	2612
88	Response	SS1.41.X-	g	999	mV/EU	Voltage	3701M15	8175
89	Response	SS1.20.R	g	999	mV/EU	Voltage	3701M15	8157
90	Response	SS1.20.T	g	997	mV/EU	Voltage	3701M15	2582
91	Response	SS1.21.R	g	990	mV/EU	Voltage	3701M15	8156
92	Response	SS1.21.T	g	985	mV/EU	Voltage	3701M15	8171
93	Response	SS1.46.X	g	996	mV/EU	Voltage	3701G3FA3G	3021
94	Response	SS1.46.R-	g	990	mV/EU	Voltage	3701G3FA3G	2028
95	Response	SS1.46.T	g	998	mV/EU	Voltage	3701G3FA3G	2029
96	Response	SS1.47.X	g	993	mV/EU	Voltage	3701G3FA3G	3051
97	Response	SS1.47.R-	g	998	mV/EU	Voltage	3701G3FA3G	3025
98	Response	SS1.47.T	g	1000	mV/EU	Voltage	3701G3FA3G	3022
99	Response	SS1.48.X-	g	694	mV/EU	Voltage	3711D1FA3G	518
100	Response	SS1.48.R-	g	696	mV/EU	Voltage	3711D1FA3G	519
101	Response	SS1.49.X-	g	978	mV/EU	Voltage	3701G3FA3G	2096
102	Response	SS1.49.R-	g	982	mV/EU	Voltage	3701G3FA3G	2095

Table C.4. Acquisition Channel Setup (1 of 2)

TRANSDU	INPUT CHANNELS				
Channel	Coupling	Range	Offset	Pre-gain	Weighting
1	DC Gnd	5 V	0	1	Off
2	DC Gnd	5 V	0	1	Off
3	DC Gnd	1 V	0	1	Off
4	DC Gnd	1 V	0	1	Off
5	DC Gnd	1 V	0	1	Off
6	DC Gnd	1 V	0	1	Off
7	DC Gnd	1 V	0	1	Off
8	DC Gnd	1 V	0	1	Off
9	DC Gnd	1 V	0	1	Off
10	DC Gnd	1 V	0	1	Off
11	DC Gnd	1 V	0	1	Off
12	DC Gnd	1 V	0	1	Off
13	DC Gnd	1 V	0	1	Off
14	DC Gnd	1 V	0	1	Off
15	DC Gnd	1 V	0	1	Off
16	DC Gnd	1 V	0	1	Off
17	DC Gnd	1 V	0	1	Off
18	DC Gnd	1 V	0	1	Off
19	DC Gnd	1 V	0	1	Off
20	DC Gnd	1 V	0	1	Off
21	DC Gnd	1 V	0	1	Off
22	DC Gnd	1 V	0	1	Off
23	DC Gnd	1 V	0	1	Off
24	DC Gnd	1 V	0	1	Off
25	DC Gnd	1 V	0	1	Off
26	DC Gnd	1 V	0	1	Off
27	DC Gnd	1 V	0	1	Off
28	DC Gnd	1 V	0	1	Off
29	DC Gnd	1 V	0	1	Off
30	DC Gnd	1 V	0	1	Off
31	DC Gnd	1 V	0	1	Off
32	DC Gnd	1 V	0	1	Off
33	DC Gnd	1 V	0	1	Off
34	DC Gnd	1 V	0	1	Off
35	DC Gnd	1 V	0	1	Off
36	DC Gnd	1 V	0	1	Off
37	DC Gnd	10 V	0	1	Off
38	DC Gnd	1 V	0	1	Off
39	DC Gnd	1 V	0	1	Off
40	DC Gnd	1 V	0	1	Off
41	DC Gnd	10 V	0	1	Off
42	DC Gnd	10 V	0	1	Off
43	DC Gnd	10 V	0	1	Off
44	DC Gnd	10 V	0	1	Off
45	DC Gnd	1 V	0	1	Off
46	DC Gnd	1 V	0	1	Off
47	DC Gnd	1 V	0	1	Off
48	DC Gnd	100 mV	0	1	Off
49	DC Gnd	100 mV	0	1	Off
50	DC Gnd	100 mV	0	1	Off
51	DC Gnd	100 mV	0	1	Off

Table C.4. Acquisition Channel Setup (2 of 2)

TRANSDU	INPUT CHANNELS				
Channel	Coupling	Range	Offset	Pre-gain	Weighting
52	DC Gnd	100 mV	0	1	Off
53	DC Gnd	100 mV	0	1	Off
54	DC Gnd	100 mV	0	1	Off
55	DC Gnd	100 mV	0	1	Off
56	DC Gnd	100 mV	0	1	Off
57	DC Gnd	100 mV	0	1	Off
58	DC Gnd	100 mV	0	1	Off
59	DC Gnd	100 mV	0	1	Off
60	DC Gnd	100 mV	0	1	Off
61	DC Gnd	500 mV	0	1	Off
62	DC Gnd	100 mV	0	1	Off
63	DC Gnd	100 mV	0	1	Off
64	DC Gnd	100 mV	0	1	Off
65	DC Gnd	100 mV	0	1	Off
66	DC Gnd	100 mV	0	1	Off
67	DC Gnd	100 mV	0	1	Off
68	DC Gnd	100 mV	0	1	Off
69	DC Gnd	100 mV	0	1	Off
70	DC Gnd	100 mV	0	1	Off
71	DC Gnd	100 mV	0	1	Off
72	DC Gnd	100 mV	0	1	Off
73	DC Gnd	100 mV	0	1	Off
74	DC Gnd	1 V	0	1	Off
75	DC Gnd	500 mV	0	1	Off
76	DC Gnd	500 mV	0	1	Off
77	DC Gnd	1 V	0	1	Off
78	DC Gnd	10 V	0	1	Off
79	DC Gnd	10 V	0	1	Off
80	DC Gnd	10 V	0	1	Off
81	DC Gnd	10 V	0	1	Off
82	DC Gnd	10 V	0	1	Off
83	DC Gnd	1 V	0	1	Off
84	DC Gnd	1 V	0	1	Off
85	DC Gnd	1 V	0	1	Off
86	DC Gnd	1 V	0	1	Off
87	DC Gnd	1 V	0	1	Off
88	DC Gnd	1 V	0	1	Off
89	DC Gnd	1 V	0	1	Off
90	DC Gnd	1 V	0	1	Off
91	DC Gnd	1 V	0	1	Off
92	DC Gnd	1 V	0	1	Off
93	DC Gnd	1 V	0	1	Off
94	DC Gnd	1 V	0	1	Off
95	DC Gnd	1 V	0	1	Off
96	DC Gnd	1 V	0	1	Off
97	DC Gnd	1 V	0	1	Off
98	DC Gnd	1 V	0	1	Off
99	DC Gnd	1 V	0	1	Off
100	DC Gnd	1 V	0	1	Off
101	DC Gnd	1 V	0	1	Off
102	DC Gnd	1 V	0	1	Off

Table C.5. Channel Connectivity (1 of 2)

	SIGNAL CONDITIONER CHANNELS					PATCH PANEL			VXI CHANNELS	
Channel	Box	Channel	Type	Cable	Connector	Box	Channel		Card	Group
1	1	1	ICP	BNC		1	1		1	1
2	1	2	ICP	BNC		1	2		1	1
3	2	3	Capacitive	BNC		1	3		1	1
4	2	4	Capacitive	BNC		1	4		1	1
5	2	5	Capacitive	Agilent	2				1	2
6	2	6	Capacitive	Agilent	2				1	2
7	2	7	Capacitive	Agilent	2				1	2
8	2	8	Capacitive	Agilent	2				1	2
9	2	9	Capacitive	Agilent	3				1	3
10	2	10	Capacitive	Agilent	3				1	3
11	2	11	Capacitive	Agilent	3				1	3
12	2	12	Capacitive	Agilent	3				1	3
13	2	13	Capacitive	Agilent	4				1	4
14	2	14	Capacitive	Agilent	4				1	4
15	2	15	Capacitive	Agilent	4				1	4
16	2	16	Capacitive	Agilent	4				1	4
17	3	1	Capacitive	Agilent	1				2	1
18	3	2	Capacitive	Agilent	1				2	1
19	3	3	Capacitive	Agilent	1				2	1
20	3	4	Capacitive	Agilent	1				2	1
21	3	5	Capacitive	Agilent	2				2	2
22	3	6	Capacitive	Agilent	2				2	2
23	3	7	Capacitive	Agilent	2				2	2
24	3	8	Capacitive	Agilent	2				2	2
25	3	9	Capacitive	Agilent	3				2	3
26	3	10	Capacitive	Agilent	3				2	3
27	3	11	Capacitive	Agilent	3				2	3
28	3	12	Capacitive	Agilent	3				2	3
29	3	13	Capacitive	Agilent	4				2	4
30	3	14	Capacitive	Agilent	4				2	4
31	3	15	Capacitive	Agilent	4				2	4
32	3	16	Capacitive	Agilent	4				2	4
33	4	1	Capacitive	Agilent	1				3	1
34	4	2	Capacitive	Agilent	1				3	1
35	4	3	Capacitive	Agilent	1				3	1
36	4	4	Capacitive	Agilent	1				3	1
37	4	5	Capacitive	Agilent	2				3	2
38	4	6	Capacitive	Agilent	2				3	2
39	4	7	Capacitive	Agilent	2				3	2
40	4	8	Capacitive	Agilent	2				3	2
41	4	9	Capacitive	Agilent	3				3	3
42	4	10	Capacitive	Agilent	3				3	3
43	4	11	Capacitive	Agilent	3				3	3
44	4	12	Capacitive	Agilent	3				3	3
45	4	13	Capacitive	Agilent	4				3	4
46	4	14	Capacitive	Agilent	4				3	4
47	4	15	Capacitive	Agilent	4				3	4
48	4	16	Capacitive	Agilent	4				3	4
49	5	1	Capacitive	Agilent	1				4	1
50	5	2	Capacitive	Agilent	1				4	1
51	5	3	Capacitive	Agilent	1				4	1

Table C.5. Channel Connectivity (2 of 2)

	SIGNAL CONDITIONER CHANNELS					PATCH PANEL			VXI CHANNELS	
Channel	Box	Channel	Type	Cable	Connector	Box	Channel		Card	Group
52	5	4	Capacitive	Agilent	1				4	1
53	5	5	Capacitive	BNC		3	5		4	2
54	5	6	Capacitive	BNC		3	6		4	2
55	5	7	Capacitive	BNC		3	7		4	2
56	5	8	Capacitive	BNC		3	8		4	2
57	5	9	Capacitive	Agilent	3				4	3
58	5	10	Capacitive	Agilent	3				4	3
59	5	11	Capacitive	Agilent	3				4	3
60	5	12	Capacitive	Agilent	3				4	3
61	5	13	Capacitive	Agilent	4				4	4
62	5	14	Capacitive	Agilent	4				4	4
63	5	15	Capacitive	Agilent	4				4	4
64	5	16	Capacitive	Agilent	4				4	4
65	6	1	Capacitive	Agilent	1				5	1
66	6	2	Capacitive	Agilent	1				5	1
67	6	3	Capacitive	Agilent	1				5	1
68	6	4	Capacitive	Agilent	1				5	1
69	6	5	Capacitive	Agilent	2				5	2
70	6	6	Capacitive	Agilent	2				5	2
71	6	7	Capacitive	Agilent	2				5	2
72	6	8	Capacitive	Agilent	2				5	2
73	6	9	Capacitive	BNC		1	5		5	3
74	6	10	Capacitive	BNC		1	6		5	3
75	1	3	ICP	BNC		1	7		5	3
76	1	4	ICP	BNC		1	8		5	3
77	4	13	Capacitive	BNC		2	1		5	4
78	1	6	ICP	BNC		2	2		5	4
79	1	7	ICP	BNC		2	3		5	4
80	1	8	ICP	BNC		2	4		5	4
81	1	9	ICP	BNC		2	5		6	1
82	1	10	ICP	BNC		2	6		6	1
83	6	11	Capacitive	BNC		2	7		6	1
84	6	12	Capacitive	BNC		2	8		6	1
85	6	13	Capacitive	BNC		3	1		6	2
86	6	14	Capacitive	BNC		3	2		6	2
87	6	15	Capacitive	BNC		3	3		6	2
88	6	16	Capacitive	BNC		3	4		6	2
89	4	9	Capacitive	BNC		4	1		6	3
90	4	10	Capacitive	BNC		4	2		6	3
91	4	11	Capacitive	BNC		4	3		6	3
92	4	12	Capacitive	BNC		4	4		6	3
93	7	1	Capacitive	BNC		4	5		6	4
94	7	2	Capacitive	BNC		4	6		6	4
95	7	3	Capacitive	BNC		4	7		6	4
96	7	4	Capacitive	BNC		4	8		6	4
97	7	5	Capacitive	BNC		5	1		7	1
98	7	6	Capacitive	BNC		5	2		7	1
99	7	7	Capacitive	BNC		5	3		7	1
100	7	8	Capacitive	BNC		5	4		7	1
101	7	9	Capacitive	BNC		5	5		7	2
102	7	10	Capacitive	BNC		5	6		7	2

Appendix D: Data Acquisition Log

Pre-Test: Integration activities were ongoing during the pre-test days so the data will be influenced by personnel activities (pre-test data only meant for preliminary checkouts)

July 10, 2009: Finished accelerometer installation; completed data acquisition system setup and shaker installation

SS1-1: July 11, 2009; Ambient noise data with Paul and Ryan on IS-2 catwalk exciting vehicle, 128 Hz sample rate, 4 second block, 16 averages; Channels 21R and 21T had no signal; replaced high density connector with BNC's; location 20 accelerometers at angle—corrected 7/13/09

SS1-2: July 11, 2009; Burst random (~20 lb-rms), 50% of window, 128 Hz sample rate, .03125 Hz resolution, 20 averages; Some work going on in FSAM area; Channel 17 T suspect; Channels 8R and 8T have orientation swapped (corrected for 7/13/09 datasets)

SS1-3: July 11, 2009; Burst random (~20 lb-rms), 50% of window, 128 Hz sample rate, .03125 Hz resolution, 20 averages; Some work going on in FSAM area; Channel 17 T switched from channel 37 to channel 77 due to possible bad signal conditioner or VXI channel.

SS1-4: July 11, 2009; Random (~20 lb-rms), 128 Hz sample rate, .03125 Hz resolution, 20 averages; Some work going on in FSAM area; Need to check overlap processing as it was not functional for this test

SS1-5: July 11, 2009; Impact, 128 Hz sample rate, .125 Hz resolution, 5 averages; Some work going on in FSAM area; Rusty and Todd in IS-1 for impact at 41X (Run 1) and 2R (Run 2); Stepped off platform for 41X impact to minimize influence on IS-1 platform modes

July 12, 2009 Data review: confirmed need to swap 8R and 8T (also confirmed with visual inspection 7/13/09); Drive point has high response due to residual effects of shell modes >40 Hz; Preliminary mode frequencies significantly lower than predictions (attributed to unknown boundary conditions)

Test Days

SS1-6: July 13, 2009; Random (~23 lb-rms), 64 Hz sample rate, .015625 Hz resolution, 16 blocks, 31 averages with hanning window and 50% overlap; lower frequency range used to try and reduce influence of shell modes (>40 Hz); 8R and 8T not corrected for time record—corrected for FRF export; corrected labels for Run 2; Run 2 same parameters except resolution at .00781 Hz (doubled acquisition time to 34 minutes)

SS1-7: July 13, 2009; Random (~51 lb-rms), 64 Hz sample rate, .015625 Hz resolution, 16 blocks, 31 averages with hanning window and 50% overlap; Platform vibration noted at shakers; No noticeable noise in IS-1

SS1-8: July 13, 2009; Ambient, 64 Hz sample rate, .015625 Hz resolution, 16 blocks, 31 averages with hanning window and 50% overlap; Ambient data acquired during lunch break

SS1-9: July 13, 2009; Random (~40 lb-rms), Low-pass filters on force 0-40 Hz; 128 Hz sample rate, .015625 Hz resolution, 16 blocks, 31 averages with hanning window and 50% overlap

SS1-10: July 13, 2009; Sine sweep 16R-; other shaker disconnected from test article; Run 1 aborted (20 lbs-pk); Run 2-4 1.93 to 2.13 Hz at 0.02 Hz/min; Run 2 (50 lbs-pk) sweep up and down; Run 3 (100 lbs-pk) sweep up; Run 4 (150 lbs-pk) sweep up; visual motion at 50 lbs; waveform distorted (squared off at peaks) for 150 lbs

Data acquisition computer crash; data was archived prior to failure; switched to backup computer

SS1-11: July 13, 2009; Sine sweep 18R-; other shaker disconnected from test article; 1.56 to 1.72 Hz at 0.03 Hz/min; Run 1 (50 lbs-pk) sweep up and down; Run 2 (100 lbs-pk) sweep up; Run 3 (150 lbs-pk) sweep up; wave form distorted (squared off at peaks) for 150 lbs

July 14, 2009, Data Review Observations: Rocking modes at 1.6 and 2 Hz much lower than pre-test predictions (~4Hz) indicating the boundary condition was less stiff than anticipated; the weak axis corresponding to the 1.6 Hz mode lines up with shim locations 5 and 11 which had gaps prior to adding upper portion of stack (Frustum, IS-1 and IS-2); Bending modes have low MAC and orthogonality due to limited instrumentation and more compliant boundary. Therefore, the mode shape comparisons will be more qualitative; Recommendations for 2nd test day: higher amplitude random excitation (0-25 Hz range), higher resolution random (0-50 Hz range); impact tests at top of segment to identify shell/bending modes; impact tests to identify local modes near FSAM/FTS; and sine sweeps to try and better excite modes in 15-30 Hz range.

July 15, 2009: Per project request, additional accelerometers added on FSAM, FTS, and FTS battery locations (see Table 2 locations 46-49) to better define local mode response

SS1-12: July 15, 2009; Random (~95 lb-rms), 64 Hz sample rate, .0078125 Hz resolution, 15 averages with hanning window and 50% overlap; 42R impedance accelerometer had intermittent overloads; Accelerometers 48 X and R are MEMS accelerometers and appear more noisy than other channels

SS1-13: July 15, 2009; Ambient; 256 Hz sample rate, .0078125 Hz resolution, 13 averages with hanning window and 50% overlap;

SS1-14: July 15, 2009; Random (~45-50 lb-rms), 256 Hz sample rate, .0078125 Hz resolution, 25 averages with hanning window and 50% overlap;

SS1-15: July 15, 2009; Random (~50 lb-rms), 64 Hz sample rate, .0078125 Hz resolution, 31 averages with hanning window and 50% overlap;

SS1-16: July 15, 2009; Impact, 5 averages; 3% Pre-trigger; 10% force window and uniform response window; Run 1: (50R-) 90 degree location at top of Frustum from outside, 0.125 Hz resolution, 128 Hz sample rate; Run 2: (51R-) 270 degree at top of Frustum from outside, 0.125 Hz resolution, 128 Hz sample rate; For runs 3-5 two people were inside on ladders but not supported by the IS-1 platform; Run 3: (52X-) IS-1 platform on outer edge of platform along I-beam at 225 degrees, 0.125 Hz resolution, 128 Hz sample rate; Run 4: (52T-) IS-1 platform on I-

beam at 225 degrees, 0.125 Hz resolution, 128 Hz sample rate; Run 5 (52R-) radial on closeout beam for IS-1 platform at 270 degree orientation, 0.125 Hz resolution, 128 Hz sample rate; Run 6 (53X-) from inside on FSAM base plate at 120 degrees, 0.125 Hz resolution, 256 Hz sample rate; Run 7 (54R) from inside below FTS on stiffening ring radial at 65 degrees, 0.125 Hz resolution, 256 Hz sample rate; Run 8 (54X) from inside on top ring frame about 10" above FTS, 0.125 Hz resolution, 256 Hz sample rate; Run 9 (55R-) from outside 122" up from shims at ~ FSAM elevation and 150 degree angle, 0.125 Hz resolution, 256 Hz sample rate; Run 10 (56R-) from outside 84" up from shims at ~FTS location and 65 degrees, 0.125 Hz resolution, 256 Hz sample rate; Run 11 (57R) Top of frustum at 0 degrees from inside (two people inside) ,128 Hz sample rate, 0.125 Hz resolution;

SS1-17: July 15, 2009; Sine sweep 16R-; other shaker disconnected from test article; 15 to 30 Hz at 0.75 Hz/min; Run 1 (50 lbs-pk); one person stepped on shaker platform when sweep at ~17 Hz, two people on platform at ~21 Hz; Run 2 (20 lbs-pk)

NOTES OF INTEREST:

1. SS1-1 & SS1-2: open channel for DOF 17T

2. SS1-1 to SS1-5: 8R & 8T DOFS switched

3. SS1-1 to SS1-5: DOF 32R actually measuring DOF 28R

4. SS1-1 to SS1-5: People were working inside the test article during data acquisition

5. All Test Data: Data for open channels was acquired due to software requirements. This data is labeled as "Open" with a direction of 0

6. All Test Data: Data for DOFs 30X and 31X has a DC bias that could not be fully compensated for at the signal conditioner

7. SS1-6: 8R & 8T DOFS switched in time data only

8. All Test Data: 42R and 43R are impedance head accelerometers

9. Accelerometers were added to the FSAM (46 & 47), FTS battery (48), and CRD plate (49) for datasets after SS1-12

Appendix E: Test Mode Shapes

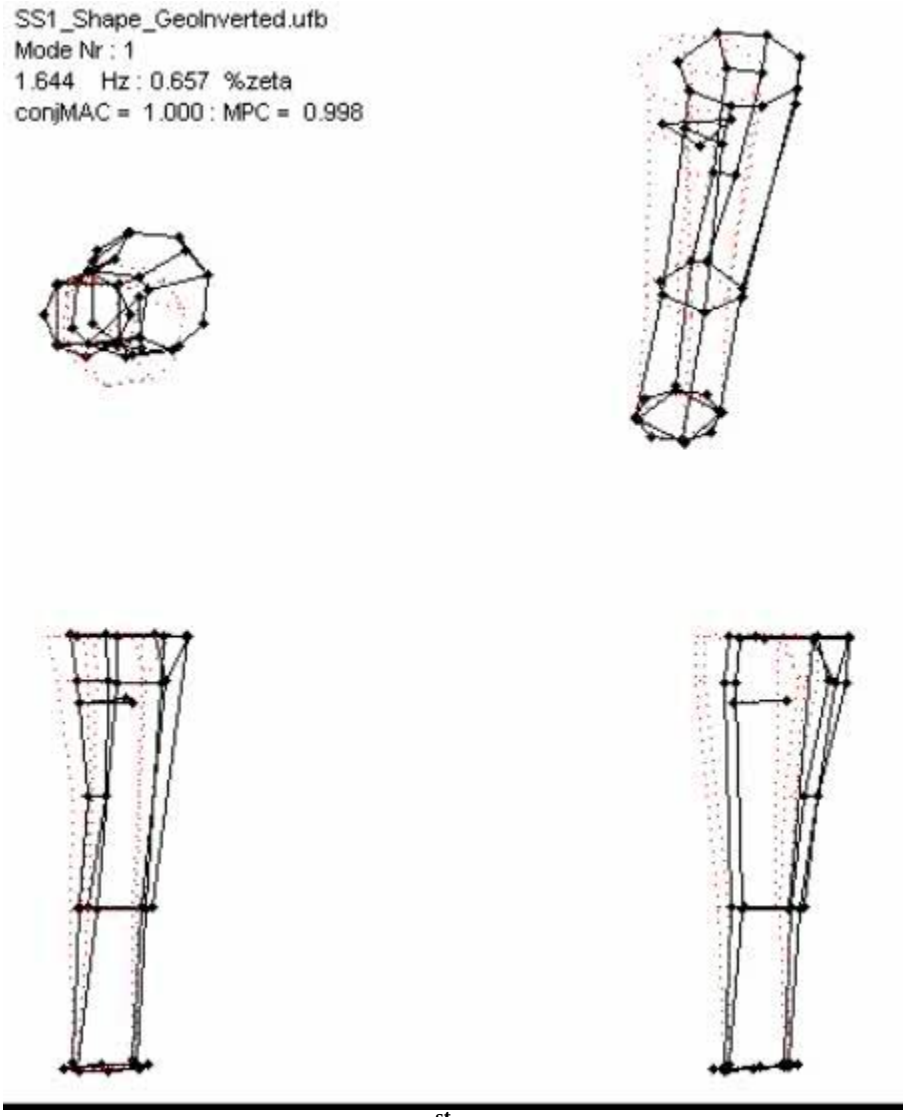

Figure E.1. Stack 1st Bending at 1.64 Hz.

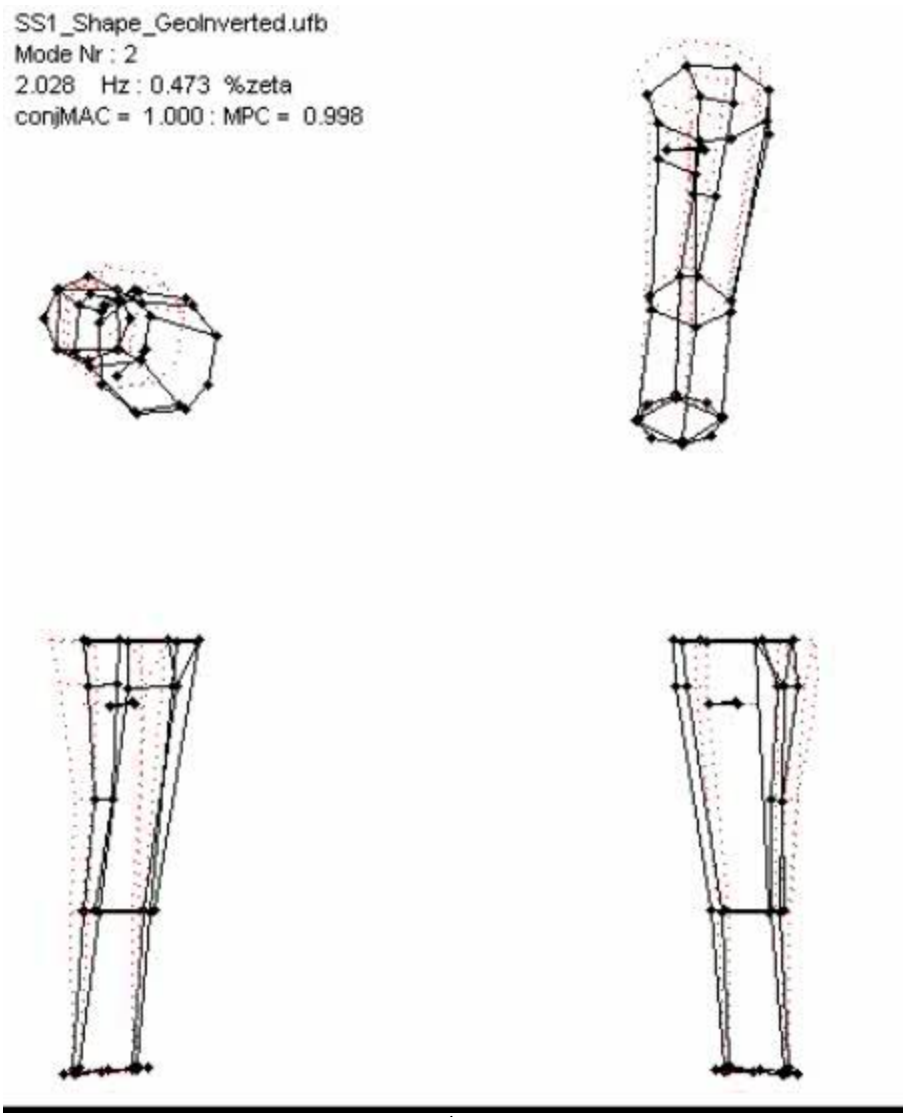

Figure E.2. Stack 1st Bending at 2.03 Hz

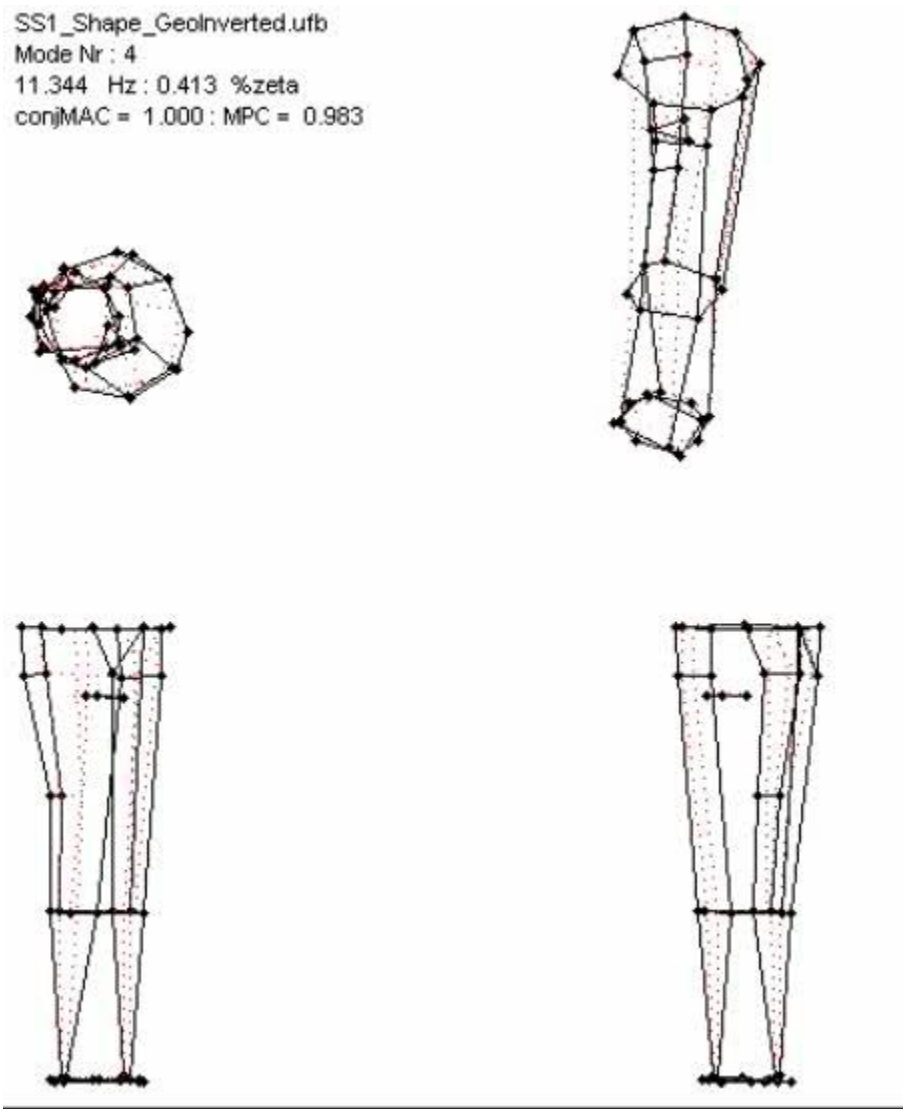

Figure E.3. Stack Torsion at 11.3 Hz

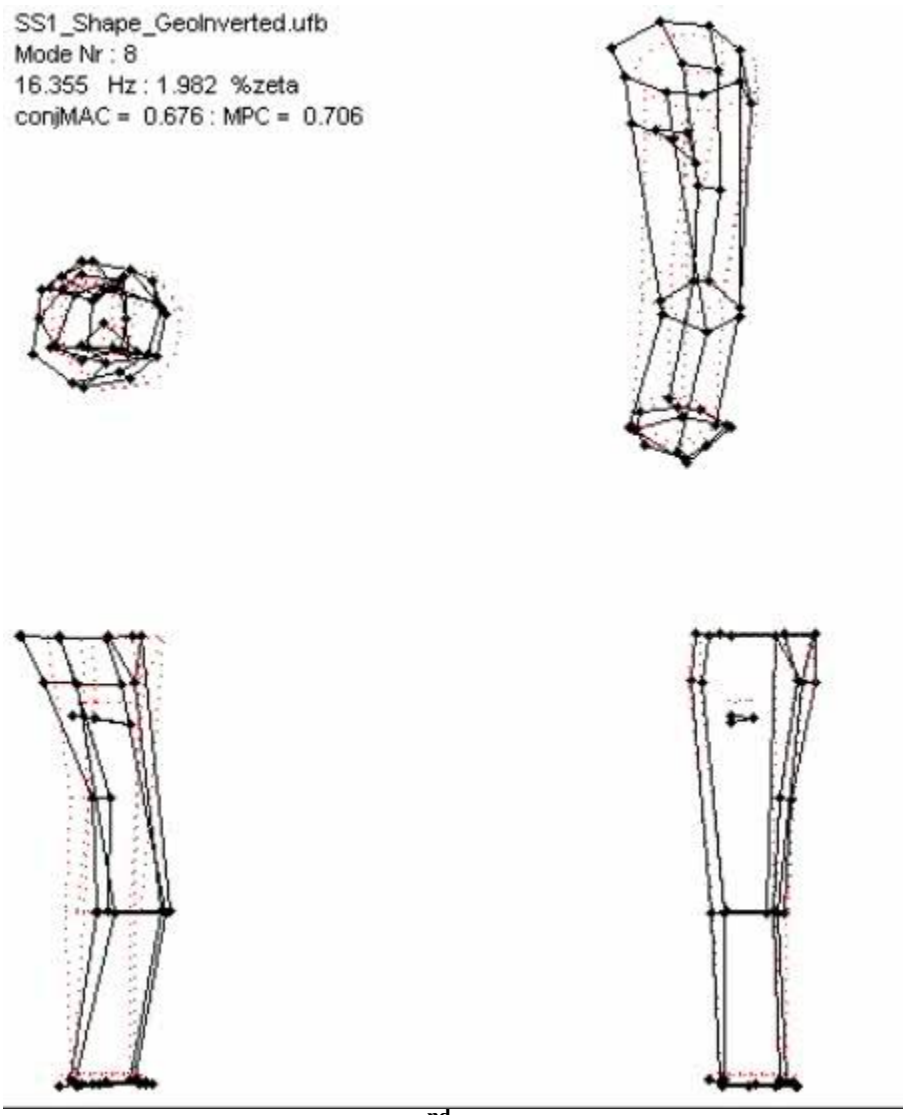

Figure E.4. Stack 2nd Bending at 16.35 Hz

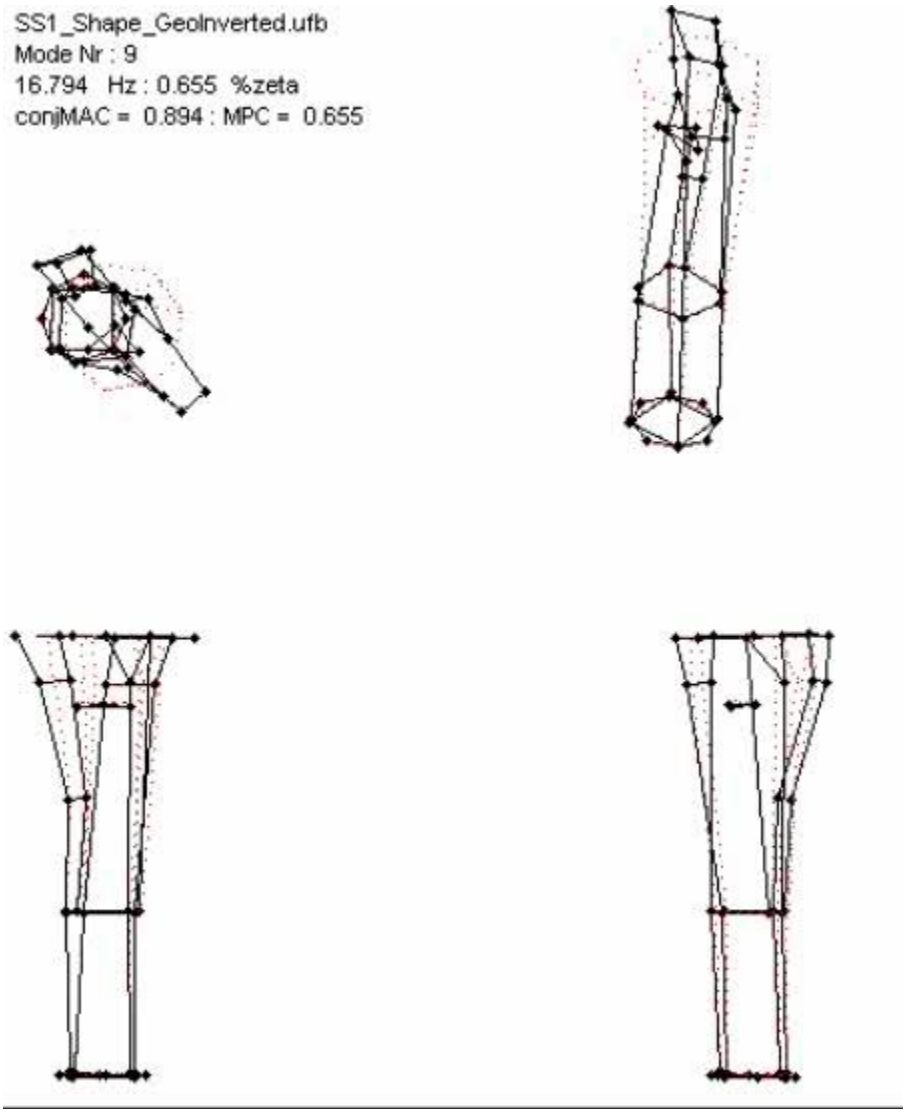

Figure E.5. 2N Shell mode at 16.8 Hz

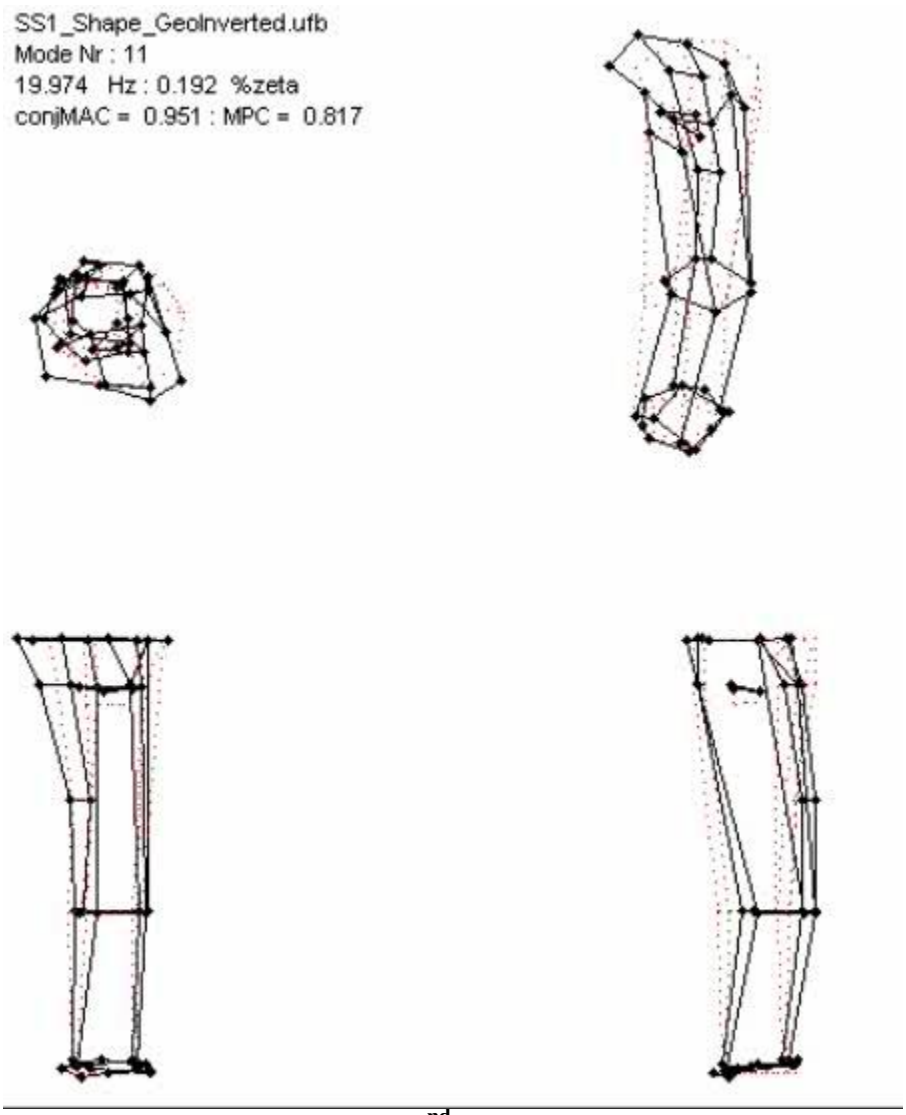

Figure E.6. Stack 2nd Bending at 19.97 Hz

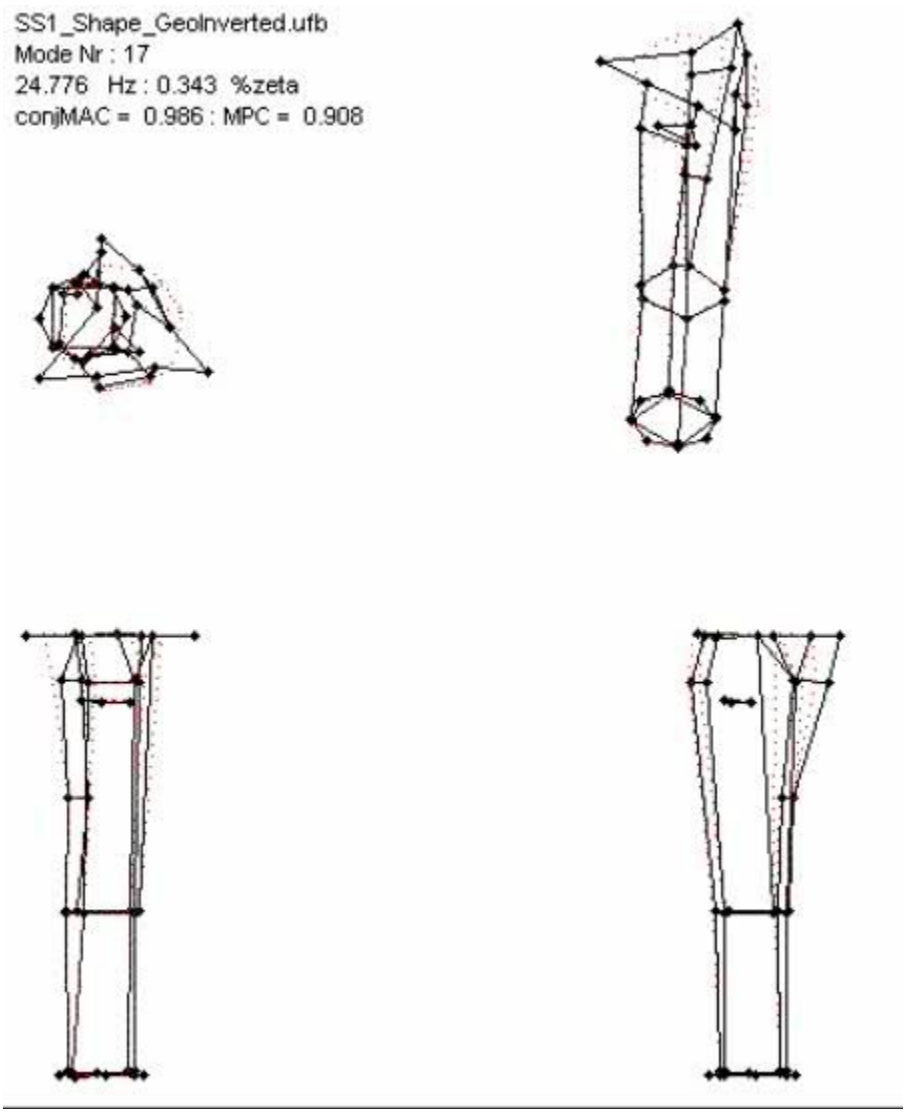

Figure E.7. 3N Shell mode at 24.8 Hz

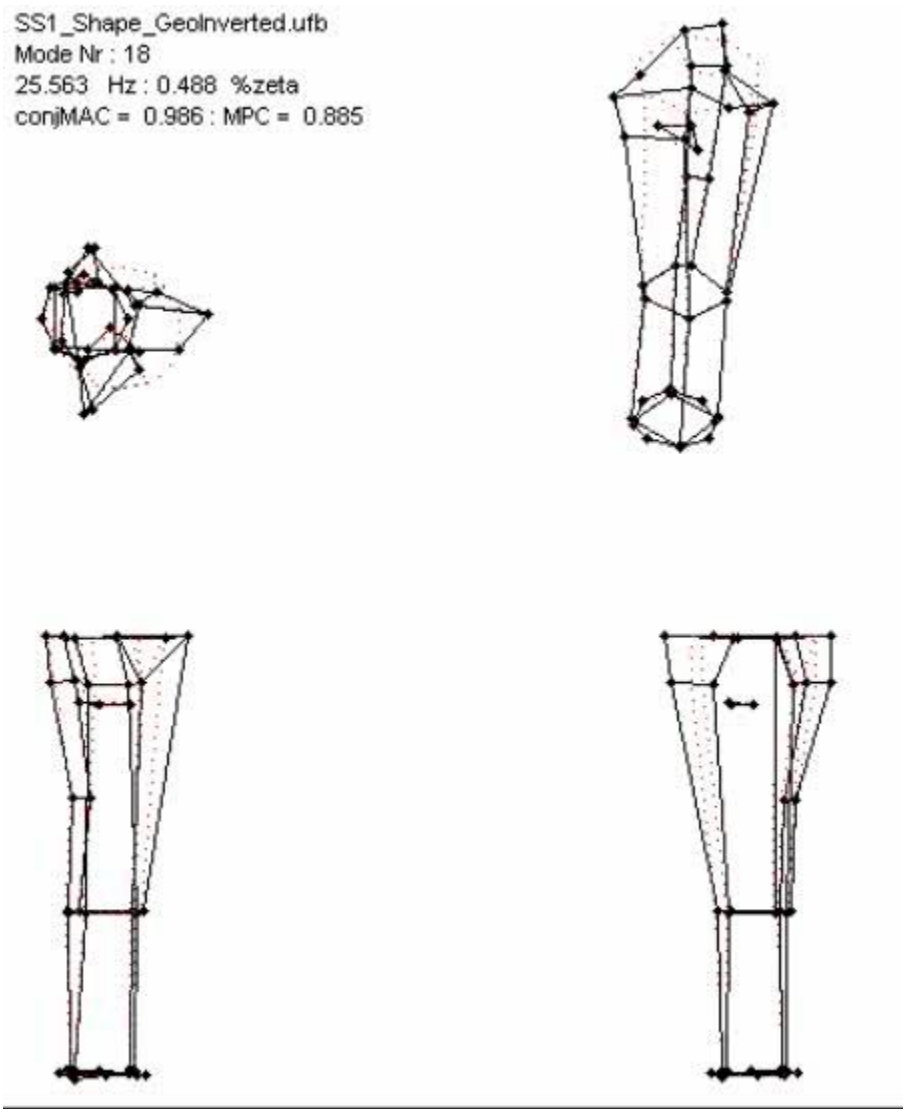

Figure E.8. 3N Shell mode at 25.6 Hz

REPORT DOCUMENTATION PAGE

Form Approved
OMB No. 0704-0188

1. REPORT DATE *(DD-MM-YYYY)*	2. REPORT TYPE	3. DATES COVERED *(From - To)*
01- 03 - 2010	Technical Memorandum	

4. TITLE AND SUBTITLE
Ares I-X Flight Test Vehicle: Stack 1 Modal Test

5a. CONTRACT NUMBER

5b. GRANT NUMBER

5c. PROGRAM ELEMENT NUMBER

6. AUTHOR(S)
Buehrle, Ralph D.; Templeton, Justin D.; Reaves, Mercedes C.; Horta, Lucas G.; Gaspar, James L.; Bartolotta, Paul A.; Parks, Russel A.; Lazor, Daniel R.

5d. PROJECT NUMBER

5e. TASK NUMBER

5f. WORK UNIT NUMBER
136905.10.10.20.20

7. PERFORMING ORGANIZATION NAME(S) AND ADDRESS(ES)
NASA Langley Research Center
Hampton, VA 23681-2199

8. PERFORMING ORGANIZATION REPORT NUMBER
L-19840

9. SPONSORING/MONITORING AGENCY NAME(S) AND ADDRESS(ES)
National Aeronautics and Space Administration
Washington, DC 20546-0001

10. SPONSOR/MONITOR'S ACRONYM(S)
NASA

11. SPONSOR/MONITOR'S REPORT NUMBER(S)
NASA/TM-2010-216210

12. DISTRIBUTION/AVAILABILITY STATEMENT
Unclassified - Unlimited
Subject Category 18
Availability: NASA CASI (443) 757-5802

13. SUPPLEMENTARY NOTES

14. ABSTRACT

Ares I-X was the first flight test vehicle used in the development of NASA's Ares I crew launch vehicle. The Ares I-X used a 4-segment reusable solid rocket booster from the Space Shuttle heritage with mass simulators for the 5th segment, upper stage, crew module and launch abort system. Three modal tests were defined to verify the dynamic finite element model of the Ares I-X flight test vehicle. Test configurations included two partial stacks and the full Ares I-X flight test vehicle on the Mobile Launcher Platform. This report focuses on the second modal test that was performed on the middle section of the vehicle referred to as Stack 1, which consisted of the subassembly from the 5th segment simulator through the interstage. This report describes the test requirements, constraints, pre-test analysis, test operations and data analysis for the Ares I-X Stack 1 modal test.

15. SUBJECT TERMS
Boundary condition; Modal parameters; Modal test; Model calibration

16. SECURITY CLASSIFICATION OF:			17. LIMITATION OF ABSTRACT	18. NUMBER OF PAGES	19a. NAME OF RESPONSIBLE PERSON
a. REPORT	b. ABSTRACT	c. THIS PAGE			STI Help Desk (email: help@sti.nasa.gov)
					19b. TELEPHONE NUMBER *(Include area code)*
U	U	U	UU	70	(443) 757-5802